Author
Monika Litviňuková

Submission
Institute of Biophysics

Thesis Supervisor
PD Dr. Rainer Schindl

Year
2016

Calcium signalling and gene regulation by carcinogenic Orai mutants

Master's Thesis

to confer the academic degree of

Master of Science

in the Master's Program

Biological Chemistry

Jihočeská univerzita
v Českých Budějovicích
University of South Bohemia
in České Budějovice

JIHOČESKÁ UNIVERZITA V ČESKÝCH BUDĚJOVICÍCH
Branišovská 1645/31a
370 05 České Budějovice,
Česká Republika
www.jcu.cz

JOHANNES KEPLER UNIVERSITÄT LINZ

JOHANNES KEPLER UNIVERSITÄT LINZ
Altenberger Straße 69
4040 Linz, Österreich
www.jku.at

JOHANNES KEPLER
UNIVERSITÄT LINZ

Sworn declaration

I hereby declare under oath that the submitted Master's Thesis has been written solely by me without any third-party assistance, information other than provided sources or aids have not been used and those used have been fully documented. Sources for literal, paraphrased and cited quotes have been accurately credited.

The submitted document here present is identical to the electronically submitted text document.

Monika Litviňuková

Acknowledgement

I would first like to thank my thesis advisor Dr. Rainer Schindl for leading me through this project. He gave me courage and motivation I needed for the work while supporting my curiosity. He always made me feel like a fellow scientist rather than just a student and appreciated my work and input. He was also always open for discussion and offered help whenever I had any questions. I couldn't have wished for a better supervisor and mentor.

I would also like to thank my other colleagues from the Ion Channel Group at the Institute of Biophysics led by Univ. Prof. Dr. Christoph Romanin for a warm welcome and for support during my project.

I would also like to acknowledge professors Prof. RNDr. Libor Grubhoffer, CSc. and Univ.-Prof. Dr. Norbert Müller for the establishment and management of the Biological Chemistry Programme.

Finally, I must express my very profound gratitude to my parents and friends for providing me with unfailing support and continuous encouragement throughout my years of study and through the process of researching and writing this thesis. This accomplishment would not have been possible without them. Thank you.

Abstract

Store operated calcium influx is one of the main Ca^{2+} pathways in many different cell types. The main representatives Orai1, the Ca^{2+} selective ion channel, and STIM1, the Ca^{2+} sensor in endoplasmatic reticulum, are essential for the activation of the immune cells. However, the effect of modified calcium signaling was previously associate with several immune system malfunctions, tubular myopathy and cancer. In this study I systematically screened for Orai1 mutants acquired form large scale cancer genomic datasets. The total of 17 mutation were investigated in the means of the channel gating using NFAT reporter assay and electrophysiological recording with the patch-clamp technique. The results of the NFAT driven RFP production yielded 8 mutants that indeed alter the channel gating and switch the protein into partially or fully open state without the need for the store depletion.The most notable result was the middle of the second trans-membrane domain which contains two of the constitutively active cancer mutants, A137V and M139V, as well as the tubular aggregate myopathy-linked L138F mutation. In addition, a neighbouring H134A mutation resulted in the largest signals of the whole set. The insertion of a spatially small alanine into this position drastically increases channel activity and allow further Ca^{2+} signaling. However, in the electrophysiological measurements only A137V generated visible constitutive signals while the other cancer mutants may produce Ca^{2+} signals below the detection limit of the patch-clamp technique. The limited constitutive Ca^{2+} influx may allow for activation of transcription, while avoiding Ca^{2+} overload which would quickly result in cell apoptosis. In this study I reveal that Orai1 cancer mutants are drivers to inducing Ca^{2+} dependent transcription and determine a central second TM helix segment of Orai1 as pivot point for the channel opening.

Abbreviations

CAD	CRAC activating domain
CaM	calmodulin
CaV	voltage gated calcium channel
CC	coiled-coil
CFP	cyan fluorescent protein
CMD	CRAC modulatory domain
CRAC	calcium release activated calcium
DAG	diacyl glycerol
DMEM	Dulbeco minimal essential medium
DNA	deribonucleic acid
DPBS	Dulbecco's Phosphate-Buffered Saline
EBSS	Earle's Balanced Salt Solution
EDTA	ethylenediaminetetraacetic acid
EGTA	ethylene glycol tetraacetic acid
ER	endoplasmic reticulum
GoF	gain of function
HEK	human embryonic kidney
HEPES	4-(2-hydroxyethyl)-1-piperazineethanesulfonic acid
IP3	inositol 1,4,5-triphosphate
LoF	loss of function
MEM	minimum essential medium
NCI	National Cancer Institute
NFAT	nuclear factor of activated T cells
NMR	nuclear magnetic resonance
OASF	Orai activating small fragment
PIP2	phosphatidylinositol 4,5-bisphosphate
PLC	phospholipase C
PM	plasma membrane
PTP	permeability transition pore
RBL	rat basophilic leukaemia
RFP	red fluorescent protein
SAM	sterile α motif
SCID	severe combined immunodeficiency
SERCA	sarco/endoplasmic reticulum Ca^{2+}-ATPase
SHD	STIM1 C-terminal homomerization domain
SOAP	STIM-Orai association pocket
SOAR	STIM-Orai activating region
SOC	store operated calcium channel
SOCE	store operated calcium entry
STIM	stromal interaction molecule
TAM	tubular aggregate myopathy
TG	thapsigargin
TM	trans membrane
TCR	T-cell receptor
TRP	transient receptor potential
WT	wild type
YFP	yellow fluorescent protein

1. Introduction

1.1. Calcium Signaling

Calcium ions play an important role in nearly every aspect of cellular life. Ca^{2+} flux is known to trigger both short and long term cellular responses making it responsible for variety of body functions including cell motility, secretion, muscle contraction and gene regulation (Berrige et al. 2003). The calcium signaling in a cell and its connectivity to several channels and pathways are illustrated in figure 1 (Nowycky and Andrew 2002). The Ca^{2+} ion is an important messenger included in numerous processes of the cell including various organelles.

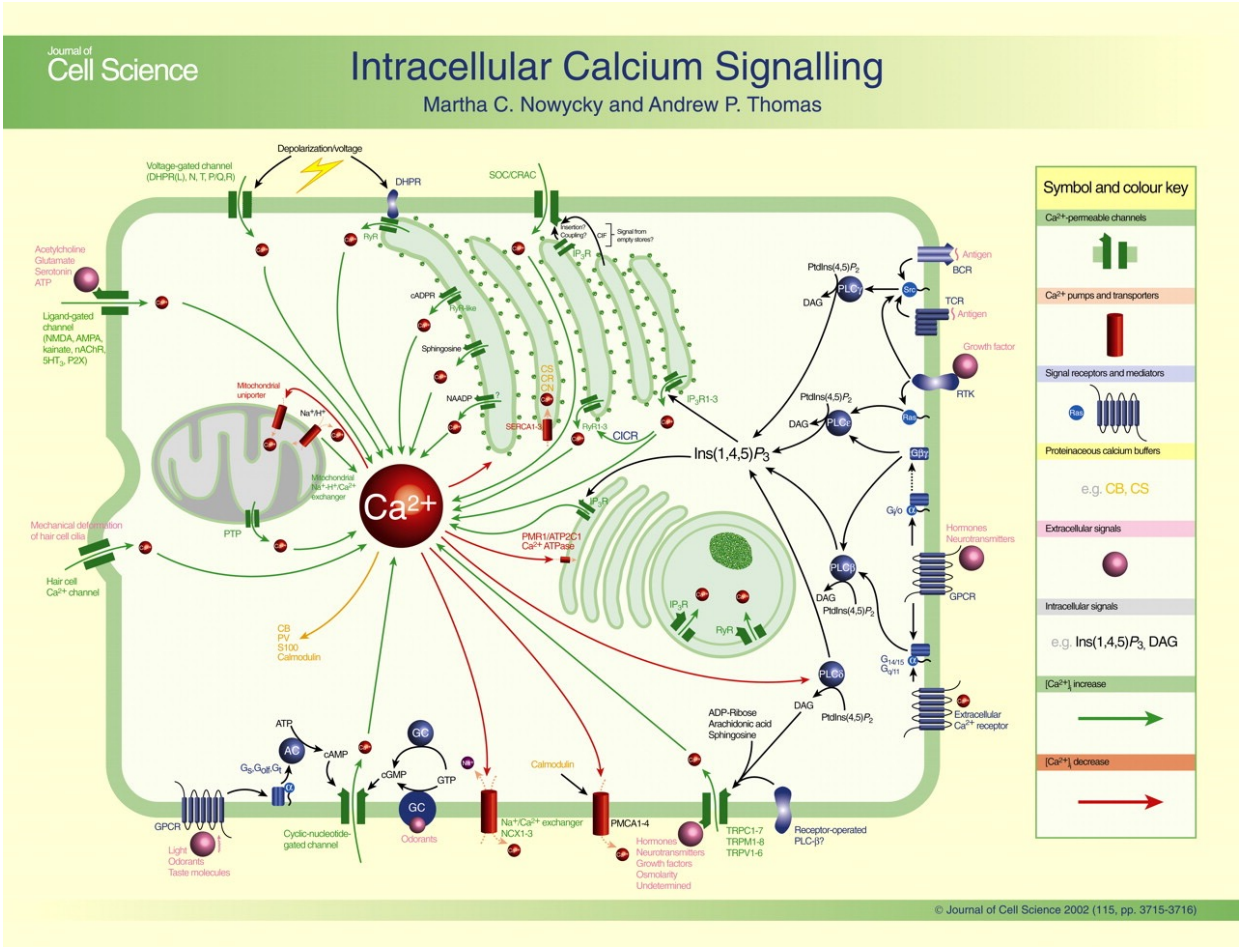

Figure 1: Calcium signaling in a cell. Calcium transport is facilitated through plasma membrane (via store-operated channels, CaV, TRP channels and others) as well as in endoplasmatic reticulum (via IP_3 receptors, SERCA pumps and other systems) and mitochondria (via PTP and mitochondrial channels). The symbol key shows the different graphics for Ca^{2+} channels and pumps, signal receptors and also both extra- and intracellular responses to Ca^{2+} signal. The change in Ca^{2+} concentration is noted by green arrow (increase) and red arrow (decrease). (Nowycky and Andrew 2002)

The calcium entry into the cell is facilitated by the diverse ion channels and the flux itself is driven by the Ca^{2+} gradient formed across the plasma membrane. The intracellular Ca^{2+} concentration is commonly around 100 nM where the extracellular levels are in the mM range. The extracellular calcium concentration is closely related to the cell location and environment. Most of the cells in a human body are exposed to approximately 2 mM Ca^{2+} concentration but in some cases, as in basal epidermal layer, the concentration is only 0.2 mM (Stanisz et al. 2012).
Calcium signals can be divided into different categories based on the triggering conditions and activation time. Voltage-gated Ca^{2+} channels (CaVs) (Fig. 1) are the fastest calcium signaling proteins. In the range of milliseconds, CaVs can increase the intracellular Ca^{2+} levels by more then 10-fold (Clapham 2007). On the other end of the calcium signaling timeline we can find store-operated Ca^{2+} channels (SOC) (Fig. 1). Those channels are able to create long-term calcium signals in a range of minutes to hours. Another calcium pathway is through transient receptor potential (TRP) ion channels (Fig. 1). In contrast to the voltage-gated and store-operated ion channels, TRP channels are non-selective for cations. Up to 27 different types of TRP channels can be found in human cells varying in activation mechanism and function (Ramsey et al. 2006).

The voltage operated channels present the crucial calcium pathways for the excitable cells. The channels can be also found in the non-excitable cells but there the signal is close to negligible compared to the SOC influx (Kotturi, Carlow et al. 2003, Kotturi and Jefferies 2005). The architecture of CaVs consists of an α1, β and α2δ subunits. The α1 subunit forms the actual pore through the plasma membrane and serves as the voltage sensor. The other two subunits are responsible for the mobility and gating of the channel (Isom, De Jongh et al. 1994, Walker and De Waard 1998). The majority of voltage-operated Ca^{2+} channels can be found in brain and heart muscle where they facilitate synaptic vesicle release and muscle contraction (Catterall 2000).

1.2.Store Operated Calcium Entry - CRAC

Store-operated Ca^{2+} entry (SOCE) is of crucial importance in variety of cells, most significantyl in the non-excitable cells, where it represents the main calcium influx. Store-operated Ca^{2+} channels can be also found in excitable cells but in the low expression. Their contribution to Ca^{2+} signalling processes in this type of cells is insignificant compared to the voltage-gated channels (Lyfenko and Dirksen 2008, Stiber, Hawkins et al. 2008).
Ca^{2+} release-activated Ca^{2+} (CRAC) channels can be considered a classical model for SOCE. The CRAC channel is formed by a two-component system of a stromal interaction molecule (STIM) and an Orai pore. The activity of the channel is directly linked to the calcium concentration inside the endoplasmatic reticulum (ER). The change of the Ca^{2+} concentration is sensed by the STIM

protein. Upon depletion of the stores the STIM translocates towards the plasma membrane (PM) and forms puncta with the Orai channel there. STIM-Orai interaction is followed by the channel rearrangement and Ca^{2+} influx.
The main characteristics of CRAC channels are their high selectivity for Ca^{2+}, low single channel conductance and low permeability for large cations like Cs^{+} (Hoth and Penner 1993).

The immune system is closely linked to calcium signaling. The store-operated calcium channels regulate the T-lymphocyte activation, mast cell degranulation and gene expression of cells. One of the responses to the CRAC activation is a cytokine secretion as an early stage of immune responses (Feske 2007, Oh-hora and Rao 2008). The severe immunodeficiency syndrome was also previously linked to the SOC. Those patients exhibit a loss of the store-operated Ca^{2+} influx due to the R91W mutation in the Orai1 channel (Feske, Gwack et al. 2006)

1.2.1. STIM

The stromal interaction molecule (STIM) is located on the ER membrane with extensions to the cytosol and the ER lumen. The main function of this protein lies in sensing the Ca^{2+} concentration inside the ER and mediating its drop to the Orai channel on the plasma membrane (Parekh and Putney 2005). The STIM occurs in two homologs, STIM1 and STIM2. In this thesis I focus on the STIM1 molecule exclusively. Each STIM1 molecule is formed by a calcium-sensing EF hand, sterile α motif (SAM), transmembrane domain and three coiled-coil regions with Orai binding site. The structure can be seen in figure 2.

The N terminus with its two main domains, EF hand and SAM, is located inside the ER lumen. The EF hand is the calcium binding site and as long as calcium is bound, the molecule resides in the resting state (Stathopulos et al. 2008). The function of the SAM region takes place during multimerization upon activation. The N terminus structure was resolved using NMR and is shown in figure 3. EF hand and SAM are highly conserved along species (Collins and Meyer 2011). Human STIM exhibits more than 85% sequence similarity with other eukaryotic species.

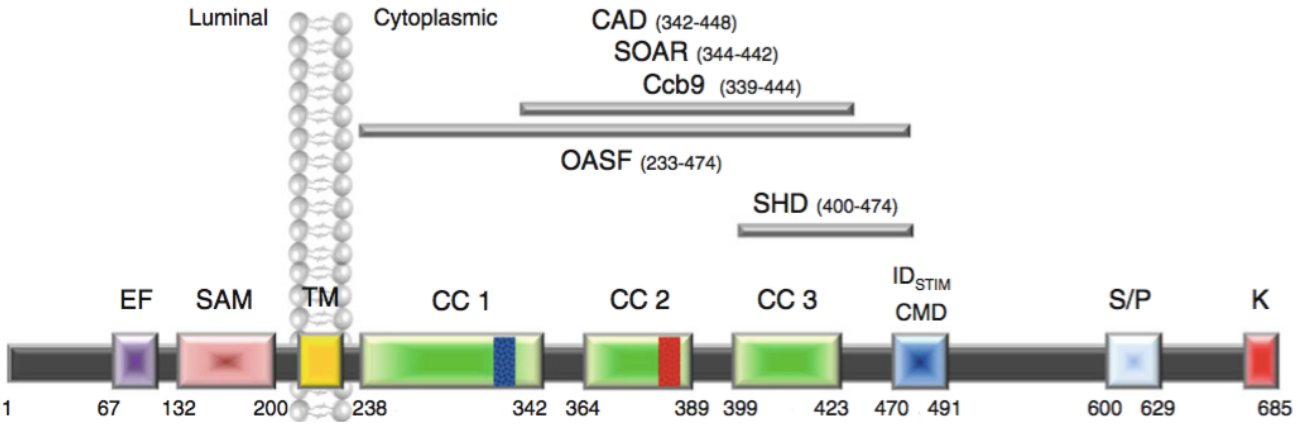

Figure 2: Structure of a STIM1 molecule: from left EF hand (EF), sterile α motif (SAM), transmembrane region (TM), coiled coil domains 1-3 (CC1, CC2, CC3), CRAC modulatory domain (CMD), serine/proline-rich domain (S/P) and lysine cluster (K). CAD, SOAR, Ccb9 and OASF are STIM1 fragments that bind Orai1 constitutively (Muik et al. 2012)

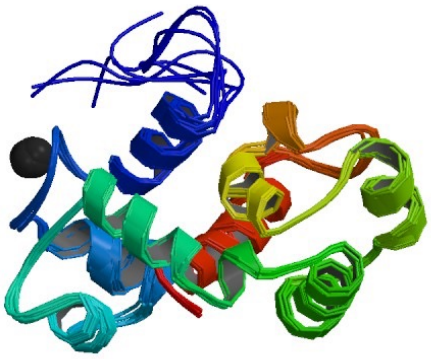

Figure 3: The N terminus of a STIM1 (PDB ID: 2K60) with a bound Ca^{2+} molecule (black) to an EF-hand domain and a sterile α motif (Stathopulos et al. 2008)

Cytosolic C terminus of the STIM1 molecule consists of three coiled-coil domains CC1, CC2 and CC3, followed by a serine/proline-rich region and a poly-lysine cluster at the end as depicted in figure 2. The CRAC modulatory domain (CMD) was found to be responsible for the inactivation of the STIM1 molecule and thus forms an important segment for the function modulation (Derler et al. 2009)

Different regions of the C terminus were previously labeled for its function. The CC1-CC3 can be referred to as an Orai activating small fragment (OASF) with residues 233-474. The OASF was previously proved to be able to activate the Orai channel without store depletion (Muik, Fahrner et al. 2009) thus earning its name. The STIM-Orai activating region (SOAR) with residues 344-442

(Yuan et al. 2009), CRAC activating domain (CAD) with residues 342-448 (Park et al. 2009) and Ccb9 with residues 339-444 (Kawasaki, Lange and Feske 2009) were also determined as being able to fully activate the SOCE without store depletion. The structure of the SOAR region was resolved using x-ray diffraction and can be seen in figure 4 (Yang et al. 2012). Residues 421-474 were determined to be crucial for STIM1 oligomerization and the segment was named STIM1 C-terminal homomerization domain (SHD). In the absence of SHD, cytosolic STIM1 fails to oligomerize and remains as a monomer (Muik et al. 2009).

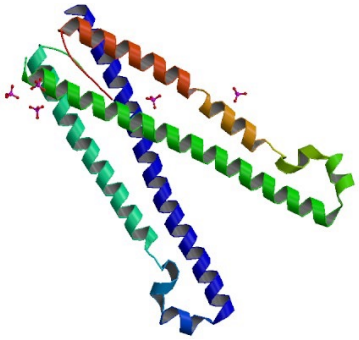

Figure 4: The dimer of the SOAR domain formed by an R-shaped helix formation of CC2 and CC3 of STIM1 (PDB ID: 3TEQ) (Yang et al. 2011)

The STIM1-Orai binding is mediated by a creation of a STIM-Orai association pocket (SOAP) created by the CC2 and CC2' helices of the STIM dimer and their supercoiling to the Orai termini (Stathopulos et al. 2013). The structure locks the CC3 domain and might therefore allow binding to the C-terminus of Orai1. The structure of the SOAP was solved using liquid NMR and is shown in figure 5 (Stathopulos et al. 2013).

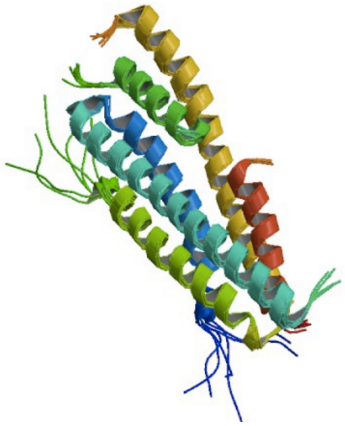

Figure 5: The STIM-Orai association pocket (SOAP) structure. The short helical Orai C-termini are shown as a green and red helix. (PDB ID: 2MAK) (Stathopulos et al 2013)

1.2.2. ORAI

The Orai is the second component of the CRAC channel and resides on the plasma membrane and serves as the pore for the calcium entry into the cell. The Orai protein was originally discovered due to its link to the severe combined immunodeficiency (SCID). In 1990s it was discovered that SCID is caused by the abolished CRAC function in the patients (Feske et al 2001). The screening discovered a previously uncharacterised membrane protein that was later named Orai1. The Orai1 mutation R91W was described to abolish the calcium currents to the cells and to be responsible for the SCID disorder (Feske at al 2006).

Orai was found to occur in three homologs: Orai1, Orai2 and Orai3. All three proteins are highly similar in sequence and structure (~62% overall identity and up to 92% identity in the transmembrane domains) but lack similarity to other ion channels making their discovery rather challenging (Prakriya and Lewis 2015). All three homologs can be found in the human genome but the Orai1 shows the largest abundance and is also the most studied of the family.

The Orai1 monomer is 33 kDa large and is formed by 4 transmembrane helices (TM 1-4) connected by flexible loops with both N and C termini facing inside of the cell. The schematics of the protein can be seen in figure 6 (Prakriya and Lewis 2015).

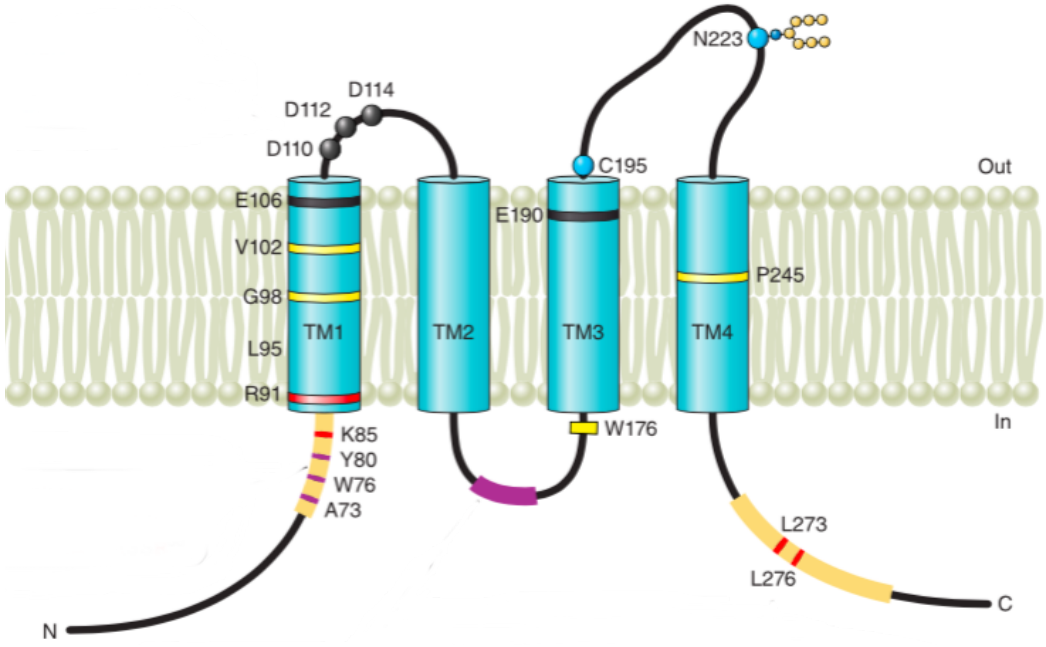

Figure 6: The structural organization of Orai1 with highlighted functional residues showing four trans-membrane domains and cytosolic N- and C-terminus(Prakriya and Lewis 2015)

The crystal structure of the Orai1 protein was resolved in 2012 from *Drosophila melanogaster* with resolution of 3.35Å. There is a high similarity to the human Orai1 as the sequence identity reaches up to 73% in transmembrane regions (Hou et al. 2012). The crystal structure solved the controversy considering the shape of the channel as previously it was believed that Orai1 subunits form a tetramer (Penna et al. 2008) but the crystal structure shows a symmetrical hexameric structure with three-fold symmetry. For the structure see figure 7.

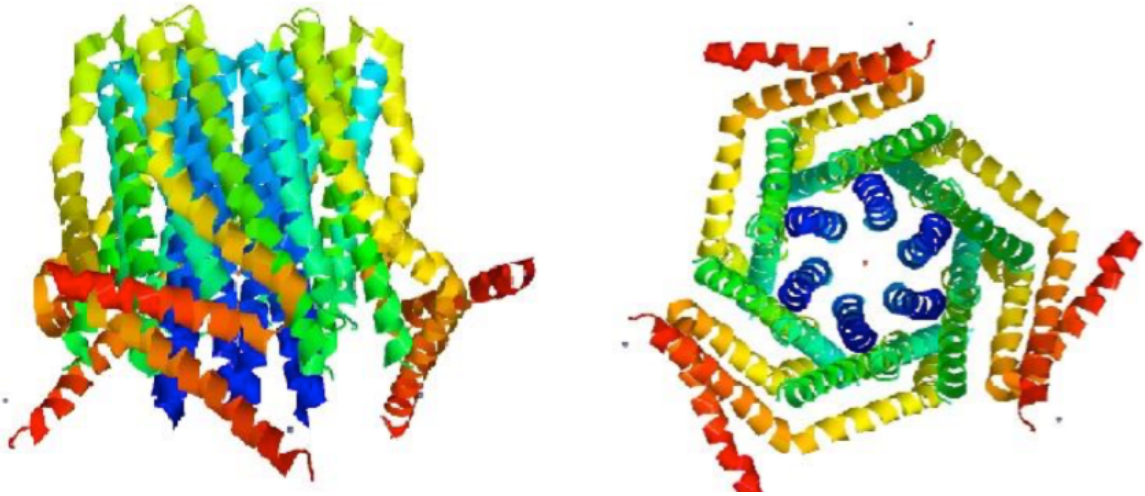

Figure 7: The crystal structure of the Orai1 (PDB ID: 4HKR), side view or the channel (left) and the orthogonal view from the intracellular side(right), pore forming TM1 (blue), TM2 and TM3 (green) and TM4 with two alternating conformations (yellow and red) (Hou et al. 2012)

The centre of the molecule is formed by six TM1 helices creating the pore for the calcium pathway. The schematics of the pore can be seen in figure 8 (Hou et al. 2012).The length of the pore is approximately 55Å long with alternating width and can be divided into four sections: i) glutamate ring on top of the pore followed by ii) hydrophobic region iii) large basic part and iv) wide section opening into the cytosol (Hou et al. 2012). Three residues of an aspartic acid located above the pore entry (D110, D112 and D114) were recently proved to be responsible for the accumulating of calcium ions to increase the local Ca^{2+} concentration and increase their permeation. (Frischauf et al. 2015).

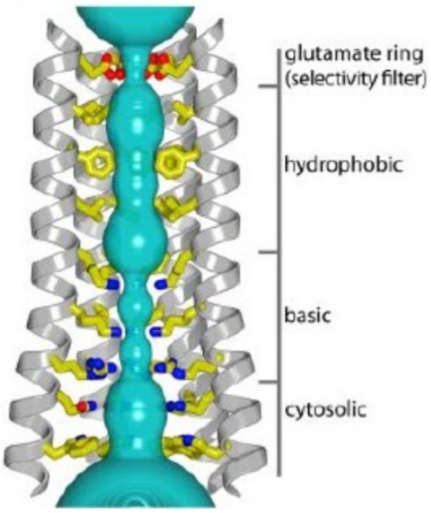

Figure 8: The pore structure derived from the resolved crystal structure highlighting the important sections for selectivity and gating. The selectivity filter is formed by a glutamate ring on top of the pore , followed by the hydrophobil and basic pore segment. (Hou et al. 2012)

On top of the pore is the ring of Glu^{106} facing inward and forming the narrowest part of the pore with diameter of ~6Å (Hou et al. 2012). Those residues form the selectivity filter and thus are responsible for the extreme Ca^{2+} selectivity (Zhou et al. 2010).
The following hydrophobic region is formed by three turns of the helices with Val^{102}, Phe^{99} and Leu^{95} facing into the pore. The width of this region is ~18Å. Point mutations in this region altered both the selectivity and the gating of the channel (Zhang, Yeromin et al. 2011, McNally, Somasundaram et al. 2012).
The basic region starts with a slight bend opening towards the cytosol and it is assumed it might be responsible for the gating of the protein. The region is three helical turns long and lining the pore with Arg^{91} Lys^{87} and Arg^{83} (Hou et al. 2012).

The pore is surrounded by a TM2 and TM3 providing the structural integrity and support of the channel (Hou et al. 2012). The outer part of the Orai1 is formed by a TM4 helices. The TM4 are unique as the helices bend outwards of the pore due to a Pro^{245}. Two alternating conformations occur at the extended TM4 and bind by coiled-coil motif forming the hydrophobic patch (Hou et al. 2012)

1.2.3.STIM-ORAI Mechanism

The store-operated Ca^{2+} entry by the CRAC channels is triggered by the direct contact of STIM and Orai molecules and thus requires close proximity of the proteins (Muik et al. 2008). This type of activation mechanism is rather unusual as the two components reside in two different cell compartments (Prakriya and Lewis 2015).

The mechanism of the CRAC channel activation can be illustrated using an example of the T cell activation (figure 9 and 10) (Hogan et al. 2010). As the resting T cell comes in contact with an antigen-presenting cell, the T cell receptors (TCR) mobilise the phospholipase C (PLC). The properties of PLC allow the cleavage of phosphatidylinositol 4,5-bisphosphate (PIP2) to diacyl glycerol (DAG) and inositol 1,4,5-triphosphate (IP_3) (Hilgemann et al. 2001). The molecule of IP_3 travels freely in the cytosol and binds to the IP_3 receptors on the ER membrane. The IP_3 receptors then trigger the release of Ca^{2+} out of the ER stores (Lewis 2001).

Upon the decrease of Ca^{2+} concentration in the ER, calcium is released from the EF hand of the STIM molecule, which destabilises the structure and causes the oligomerization and the conformational switch (Stathopulos, Li et al. 2006). During the conformation switch, the molecule exposes the CAD domain in order to increase its availability towards the Orai channel. It was previously shown that all three coiled-coil domains are responsible for the reorganisation into the extended conformation (Muik et al. 2011).

Orai molecules were found to relocate and form clusters on the PM upon store depletion (Luik, Wu et al. 2006). To facilitate the SOCE, both C and N termini of Orai are required. The putative coiled-coil domain of the C terminus of the Orai1 was found to be essential for the STIM-Orai interaction (Muik et al. 2008, Stathopulos et al. 2013). Mutants in this region disrupt the STIM-Orai binding and abolish the calcium entry (Navarro-Borelly et al. 2008, Muik et al. 2008, Calloway et al. 2009). Deletion of the N terminus abolishes the Ca^{2+} entry but only slightly decreases the STIM-Orai coupling, suggesting its importance in gating (Muik et al. 2008).

For the research purposes, the store operated calcium entry can be triggered by various methods. Use of Thapsigargin (TG) is the most commonly used in the fluorescence microscopy methods. TG travels freely into the cells and blocks SERCA pumps located on the ER membrane. The main function of the SERCA pumps is to refill the Ca2+ stores inside the ER. When blocked, Ca^{2+} leaks out of the ER causing a store-depletion and triggering SOCE. On the other hand, patch-clamp technique uses a passive store-depletion caused by EGTA in the pipette solution. The presence of EGTA buffers out the Ca^{2+} in the cytosol and thus triggers the SOCE. Another approach is using high concentrations of IP_3.

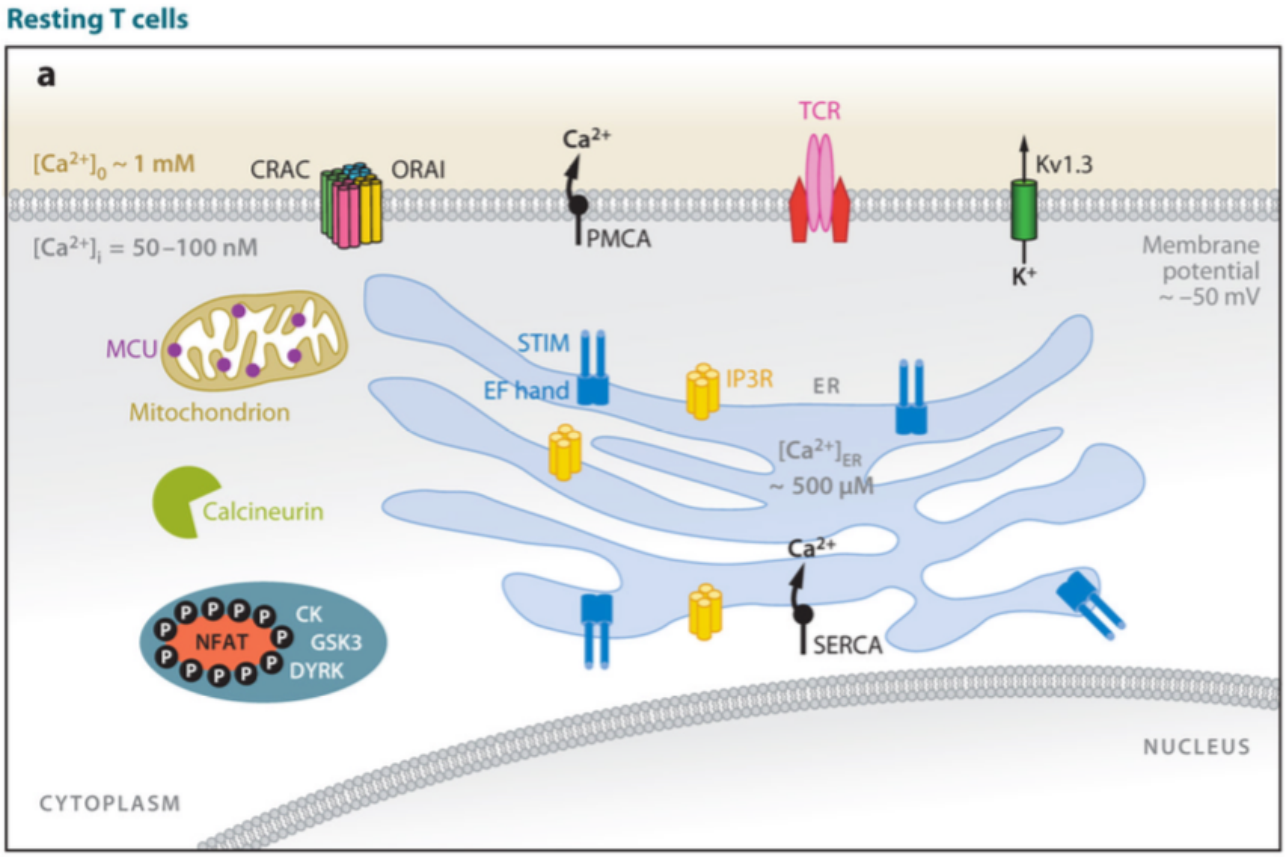

Figure 9: The organisation of a resting T cell. The T cell receptor (TCR) remains in an unbound state. STIM resides in its resting monomeric state as the Ca^{2+} concentration in the ER is maintained by SERCA pumps. Orai resides in its closed conformation in the plasma membrane. NFAT is freely present in the cytosol in its phosphorylated state. (Hogan et al 2010)

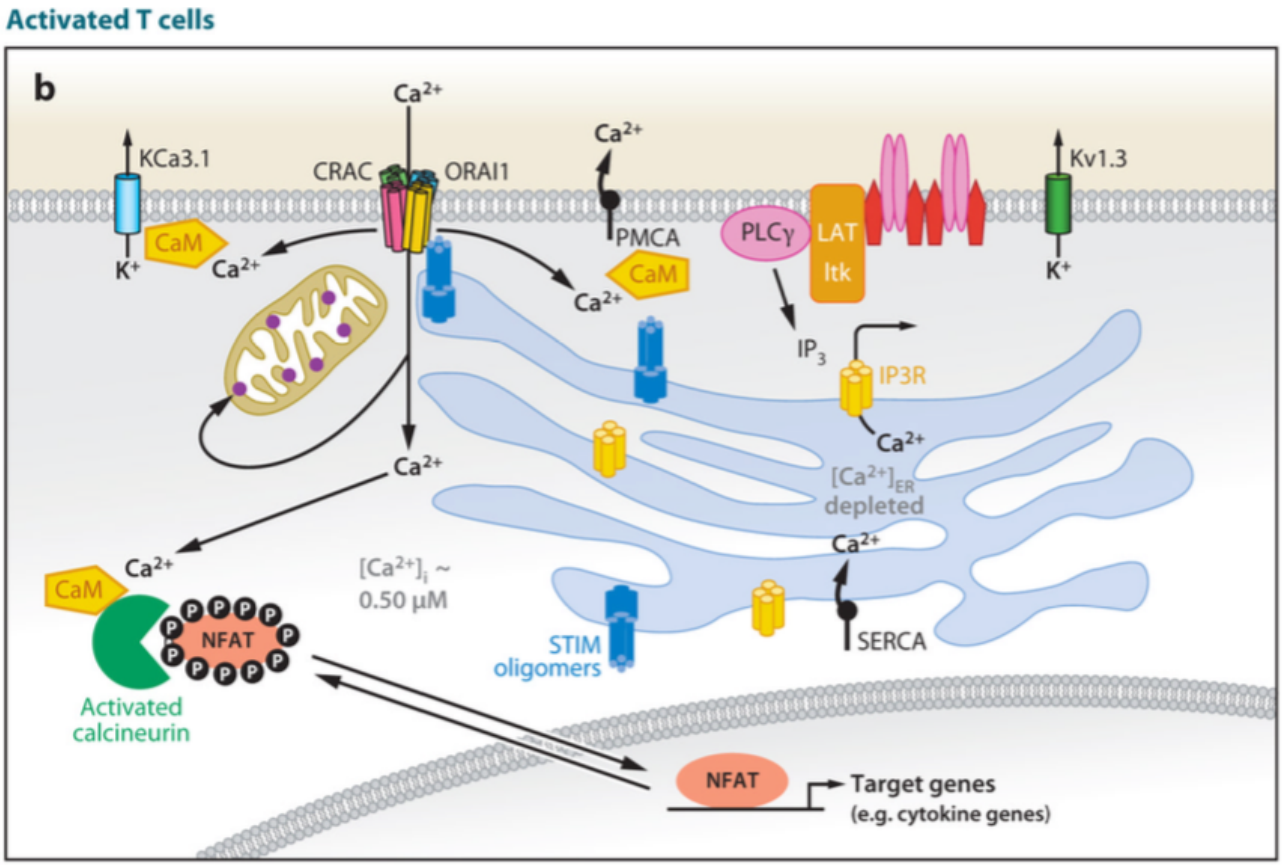

Figure 10: The organisation of the activated T cell. As a response to the outside signal, the TCR receptors assemble to a signalling complex with various proteins as LAT and phospholipase C (PLCɣ) producing inositol 1,4,5-triphosphate (IP_3). Molecules of IP_3 activate IP_3 receptors on the ER membrane and cause a drop in Ca^{2+} concentration in the ER. This triggers STIM molecules that oligomerize and travel to the PM junctions to bind to Orai molecules. The Orai facilitates the Ca^{2+} influx into the cell and activates a universal cytoplasmic Ca^{2+} sensor calmodulin (CaM). Among others, CaM binds calcineurin which later dephosphorilates NFAT and causes it to travel into the nucleus and promote transcription of certain genes. (Hogan et al. 2010)

1.2.4.NFAT activation induced by store-operated Ca^{2+} signals

After the increase of the intracellular Ca^{2+} levels, many cellular processes are triggered including calmodulin binding Ca^{2+} ions and further activation of the calcineurin proteins. Calcineurin then dephosphorylates the nuclear factor of activated T cells (NFAT) which causes its translocation into the nucleus where it enhances the transcription of specific genes and initiates a consequent immune response (Fracchia et al. 2013).

1.3.Pathophysiological Function of CRAC

Store-operated calcium channels were previously linked to many physiological and pathophysiological effects. One of the crucial SOCE discoveries, the discovery of the Orai protein, was based on the link between SOCE and severe combined immunodeficiency. The disorder was found to be caused by Orai1 R91W mutant affecting the activation of T cells and thus altering the immune system responses (Feske et al. 2006). It was also shown that patients with other defects connected to SOCE manifest various pathophysiological conditions in immunity, allergy, muscle defects and bleeding disorders (Feske 2009, Parekh 2010).

1.3.1.CRAC Channels in Disease

Mutations in both STIM and Orai were previously described to cause medical conditions. The mutations can be generally characterized by their effect on the channel function with either loss-of-function (LoF) or gain-of-function (GoF) properties. Loss-of-function mutations decrease or completely abolish the SOCE in the affected cells and are characterised by SCID-like conditions, muscular hypotonia and immunodeficiency. By contrast, gain-of-function mutations allow Ca^{2+} influx without the store depletion and result in a constitutive activity and increased calcium levels. This usually exhibits as tubular aggregate myopathy (TAM), York platelet and Stormorken syndromes (Lacruz and Feske 2015). Effects of the LoF and GoF mutations often overlap and thus underline the importance of the calcium homeostasis.

Multiple LoF mutations were defined over the years. Inherited LoF mutations of the STIM1 EF hand were found to cause tubular aggregate myopathy (Bohm et al. 2013). The STIM1 P165Q located in the SAM region is suggested to decrease dimerization ability of the protein and thus preventing the SOCE (Schaballie et al. 2015). Another non-functional STIM1 mutation located in CAD, R429C was found to disrupt SOCE and thus interfere with T cell activation (Nakamura et al. 2013). Another CAD mutation was recently discovered in position R426C and is suspected to exhibit similar effects as R429C for their close proximity in the molecule (Wang et al. 2014, Maus et al. 2015). The best described LoF Orai1 mutation is R91W. As previously mentioned, it is responsible for severe combined immunodeficiency. The crystal structure homolog to the Orai1-R91W was also resolved. In this case the pore is completely blocked due to a hydrophobic coupling of the tryptophan side-chains (Hou et al. 2012).

GoF mutants usually result in complex disease phenotypes as York or Stormorken syndrome. Stormorken syndrome is caused by autosomal-dominant STIM1 R304W mutation (Misceo et al. 2014). The mutation was described to generate close to maximal Ca^{2+} currents without store-depletion while co-expressed with the Orai1 (Nesin et al. 2014). Two families of York platelet syndrome were also linked to the R309W mutation (Markello et al. 2015). The two syndromes

share the main clinical symptoms as bleeding diathesis, thrombocytopenia, platelet defects and muscle weakness. Numerous of other STIM1 GoF mutations were reported in the TAM studies (H72Q, N80T, G81D, D84G, L96V, F108I/L, H109R/N, I115F) and showed pre-clustering or constitutive activity (Lacruz and Feske 2015). Concerning the Orai1 protein, two GoF mutations (G98S and L138F) were found to cause TAM. Those two mutants allow constitutive Ca^{2+} influx without the store depletion (Endo et al 2015). The Orai1 P245L was then found to cause Stormorken-like syndrome with TAM (Nesin et al. 2014).

The clinical symptoms resulting from the STIM1 and Orai1 point mutations highlight the importance of the proteins to the Ca^{2+} metabolism. The effects of the mutations are limited to specific tissues as platelets, immune cells, skeletal muscle and teeth but the altered CRAC channels are likely to influence other tissues as well. As the signalling pathway of STIM1 includes also other proteins as TRP channels and voltage-gated Ca^{2+} channels, the effect of its mutations might disrupt also other calcium pathways. Although the disease phenotype suggests that its main regulation function lies with Orai (Lacruz and Feske 2015).

1.3.2. CRAC Channels in Cancer

In certain types of solid tumor cancers like breast, colon or brain, on average up to 66 different genes will exhibit small somatic mutations. Those can later be responsible for the amino acid change in the protein (Vogelstein et al. 2013). Those mutations can be divided to “drivers” and “passengers”. The drivers are defined to be providing a selective growth advantage to the tumor, the passengers are the ones where direct growth advantage is not determined. A tumor will usually contain two to eight driver mutations influencing the cell fate, cell survival or genome maintenance (Vogelstein et al. 2013). The driver mutations are also characterised as the oncogenic ones, the passengers on the other hand are the ones acquired before or during cancer development (Stratton et al. 2009). It was previously reported that Ca^{2+} signals affect development, growth and metastasis of many types of cancer. CRAC genes are most likely the ones carrying the passenger mutations, whereas the combination of certain Ca^{2+} genes might form a driver (Hoth 2015).

The CRAC-mediated Ca^{2+} influx was previously associated with various carcinogenic processes as increased proliferation, suppressed apoptosis, tumor growth and metastases (Hanahan and Weinberg 2000). Several types of cancer were described to involve altered calcium signaling and homeostasis (Monteith et al. 2007). The STIM1 was proposed to have a tumor-suppressive function as its gene is deleted in the rhabdomyosarcoma. SOCE was indeed later proved to have the tumor-suppressive effect as the CRAC-mediated signals caused apoptosis of human prostate cancer cells. Androgens-regulated Orai1 expression was also described in this connection (Fluorakis et al. 2010).

On the other hand multiple studies correlate the SOCE to elevated tumor growth. Cell proliferation was found to be promoted by the SOCE in murine melanoma (Fedida-Metula et al. 2012) as well as glioblastoma (Liu et al. 2011). The studies on cervical cancer reported a correlation between tumor size and STIM1 expression where patients with increased STIM1 expression showed significantly lower five year survival rates (Chen et al. 2011). Similar results were also discovered in patients with breast cancer where high STIM1 expression resulted in decreased survival rates (McAndrew et al. 2011). Breast cancer was also associated with the elevated expression levels of Orai3 (Faouzi et al. 2011). The store-independent Ca^{2+} influx was discovered in breast cancer patients caused by Orai1 and resulting in the pathogenesis (Feng et al. 2010). SOCE was also associated with metastasis of various types of cancer (Yang et al. 2009) as well as epidermal-to-mesenchymal transition (Hu et al. 2011). Yet the full engagement of CRAC and its sub-components in the cancer development and growth was not fully elucidated. This study should bring some light into the pathophysiology of CRAC.

2. Materials and Methods

2.1.Patch Clamp

2.1.1.Theoretical Background

Patch Clamp is an electrophysiological technique focusing on the single cell measurements.The patch clamp experiment is based on the measurement of currents flowing across the plasma membrane. Those currents are generated by the opening of ion channels causing ions to flow inside or outside of the cell. Four different modes of the recordings are possible and can be achieved by different micropipette movement. Those are whole-cell, cell-attached, inside-out and outside-out and can be seen in figure 9 (modified from Hamil et al. 1981).

The whole cell recording is the most commonly used mode of the patch clamp technique. To perform such an experiment, the micropipette is brought to a close proximity of the cell and by applying small underpressure, the gigaseal is created. Next the membrane inside the micropipette tip is broken by underpressure pulse and the recording is initiated. As the pipette solution can freely mix with the cytosol, different chemicals can be delivered to initiate channel opening, e.g. EGTA for passive store depletion.

The cell-attached mode can be considered a preliminary step to the whole-cell recording. During this experiment the gigaseal is formed but the membrane is not broken and thus the recording is focused only on the membrane in the pipette-tip region. This mode is most commonly used for the single channel measurements.

The outside-out and inside-out recordings are more difficult to perform, because they rely on the membrane self-repair. The advantage of those modes is the isolation of the membrane and its channels from the rest of the cell. For the outside-out configuration the gigaseal is created and the membrane is broken. Next, the pipette tip is slowly retracted from the cell and this results in the break of the membrane from the cell. The two free ends of the membrane will then come rogether and regenerate to an outside-out patch. The inside-out mode is initiated from the cell attached mode. The gigaseal is formed and then the pipette is slowly retracted from the cell. This causes the membrane break with the inside-out patch inside of the pipette tip.

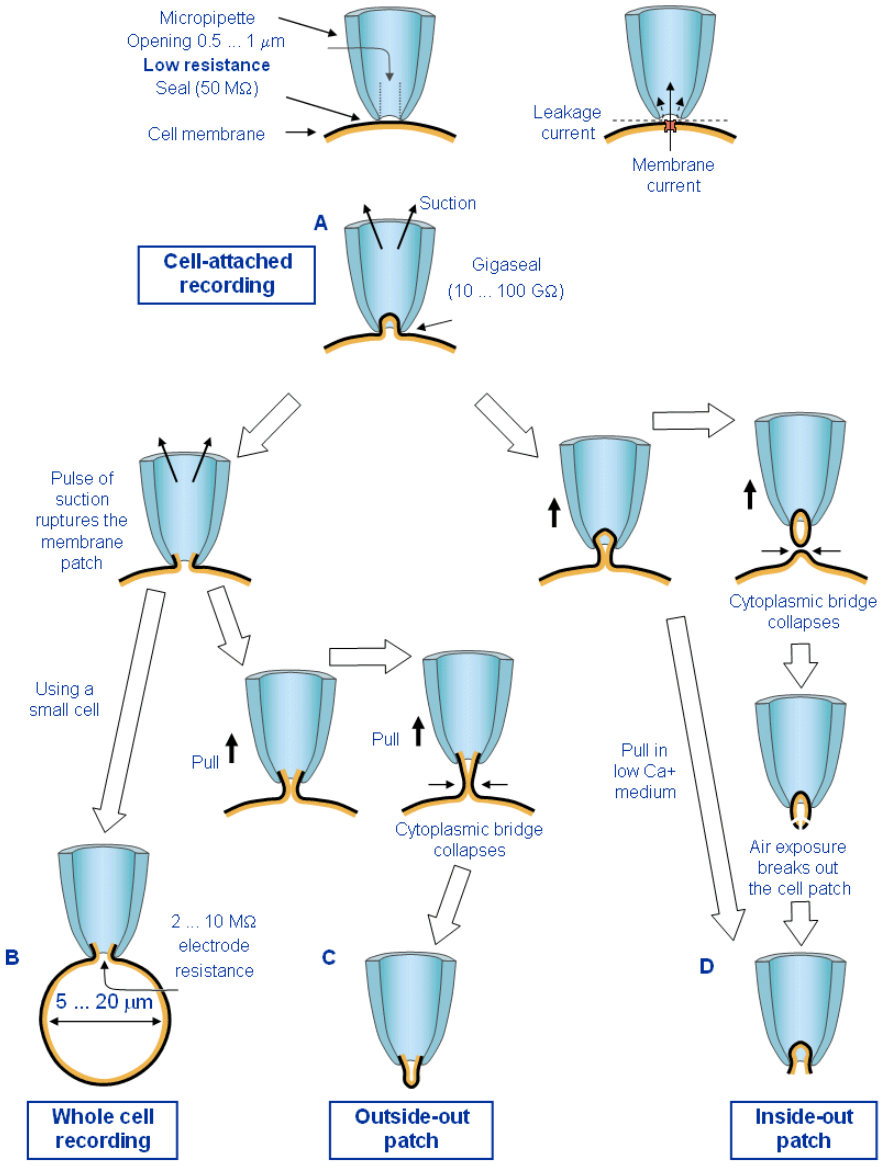

Figure 9: Four different modes of patch clamp measurements. (A) The cell attached recording, (B) the whole cell recording, (C) the outside out mode and (D) the inside out mode (modified from Hamil et al. 1981)

Patch clamp is well suited for the studies of different ion channels and their modifications. Single cells with over-expressed tagged proteins are immobilised on a glass slide in a solution containing the ions of interest and placed into a microscope. The micropipette is filled with a desired solution and a silver chloride electrode is placed inside. The reference silver chloride electrode is placed in the bath solution. Next the micropipette is brought to the close proximity of the cell using a micromanipulator and a giga-ohm seal is created. After the membrane in the pipette tip is broken using underpressure, the whole cell recording can be initiated. The experimental setup is shown in figure 10. The close-up of the patch clamp experiment is shown in figure 11 and 12.

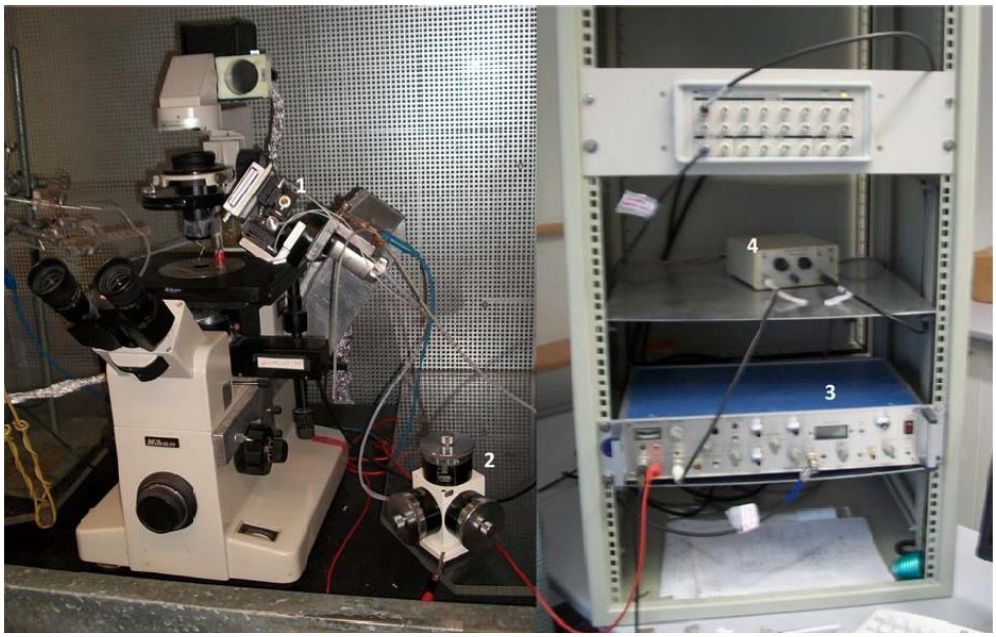

Figure 10: The experimental setup for the patch-clamp experiments containing (1) fluorescence microscope, (2) micromanipulator, (3) current amplifier and (4) low-pass amplifier

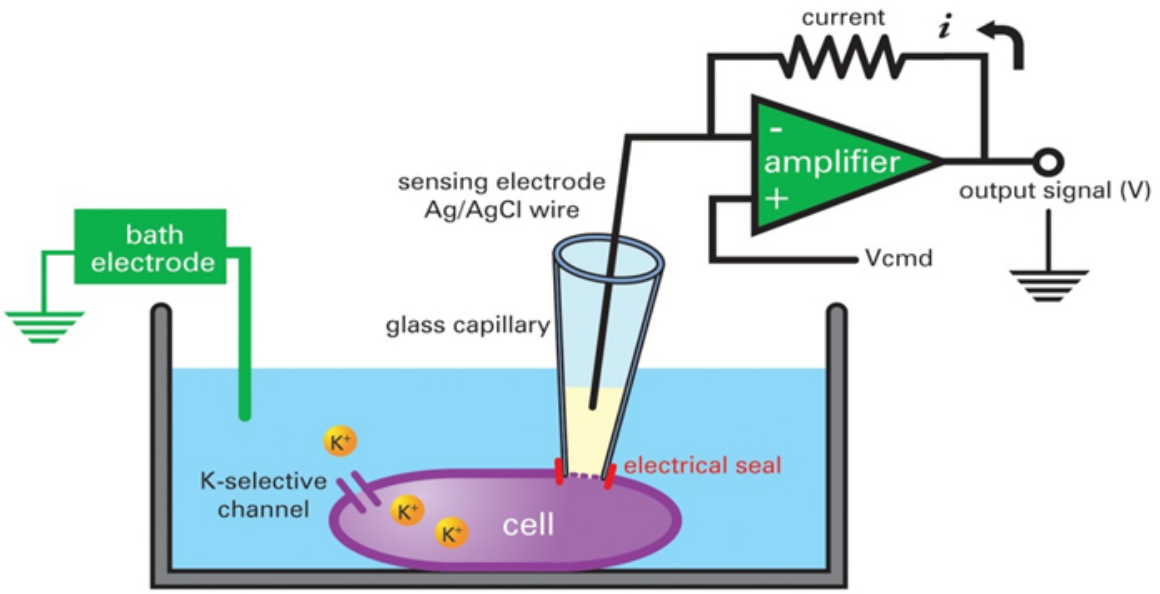

Figure 11: The diagram of the whole cell patch-clamp experiment (Clare 2010) The cells are recorded in a voltage-clamp mode when the voltage is fixed and the current flowing between the sensing intracellular electrode and the bath electrode is measured. The measured current is formed by the opening and closing of the studied channels on the plasma membrane.

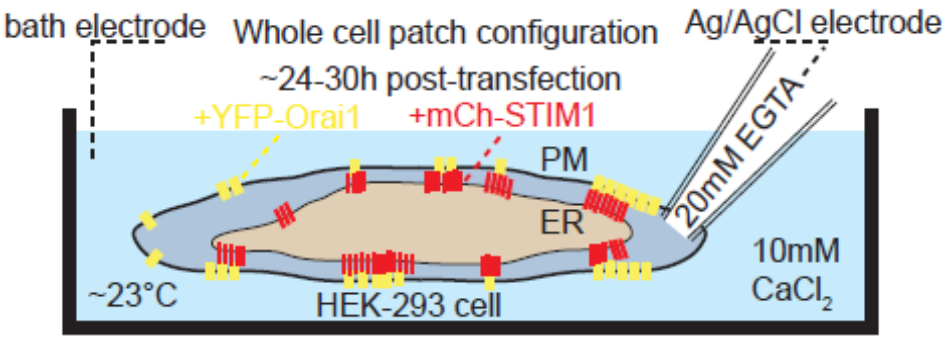

Figure 12: The illustration of the whole cell patch-clamp experiment with focus on labeled STIM1 and ORAI1 channels (Stathopulos, Schindl et al. 2013)

2.1.2. Experimental Setup

The patch clamp experiments were measured using HEK-293 cells. Those cells were transfected using TransFectin™ with 0.5-1.5 µg of YFP-Orai1 with or without 1 µg of mCherry-STIM1 constructs. To produce comparable results, the cells with similar levels of expression were measured. The cells were incubated at 37°C with 5% CO_2 atmosphere and humidity of 95% in DMEM medium and measured 24-30 hours after the transfection. All the experiments were measured at 23-25°C.

The measurement protocol consisted of repetitive voltage ramps every 5s from holding potential 0 mV covering a range from -90 to +90 mV over 1s. The pipette solution contained 20 mM of EGTA, to create a passive store depletion in order to observe SOCE. The other components of the intracellular pipette solution were 145 mM caesium methanesulfonate, 8 mM sodium chloride, 5 mM magnesium chloride and 10 mM HEPES with final pH of 7.2. The cells were placed in 10 mM Ca^{2+} extracellular solution to observe the calcium influx. The solution contained 10 mM calcium chloride, 140 mM sodium chloride, 5 mM caesium chloride, 1 mM magnesium chloride, 10 mM HEPES and 10 mM glucose with final pH of 7.4. As the cells over-expressed only the CRAC channels the obtained currents provide information exclusively about those proteins. The leak-currents were eliminated from the experiments by subtraction of either the initial current before channel activation or by subtraction of the current after application of 10 µM La^{3+} in 10 mM Ca^{2+} extracellular solution for its ability to inhibit the Orai1 currents.

2.2.NFAT Reporter Assay - Fluorescent measurements

2.2.1.Theoretical Background

The nuclear factor of activated T cells (NFAT) is a transcription factor closely related to the calcium signalling and especially SOCE. The NFAT is commonly found in its phosphorylated form in the cytosol of the cell. As the Ca^{2+} influx through SOCE appears, the calmodulin molecules are activated and transduce the signal to the phosphatase calcineurin. Calcineurin targets the NFAT molecules and dephosphorilates three of its motifs triggering its activation. The dephosphorilated NFAT shows high affinity toward its target DNA site and translocates into the nucleus where it activates the transcription (Hogan et al. 2003). The mechanism is depicted in figure 13. The effectivity of the assay was previously measured by the NFAT-triggered luciferin production but the method requires cell lysis for quantification. The transcriptional activity of the NFAT is now visualised using expression of the red fluorescent protein (RFP) which can be done directly in the microscope (Rinne and Blatter 2010). The amount or the RFP is then directly related to the activity of the CRAC channels.

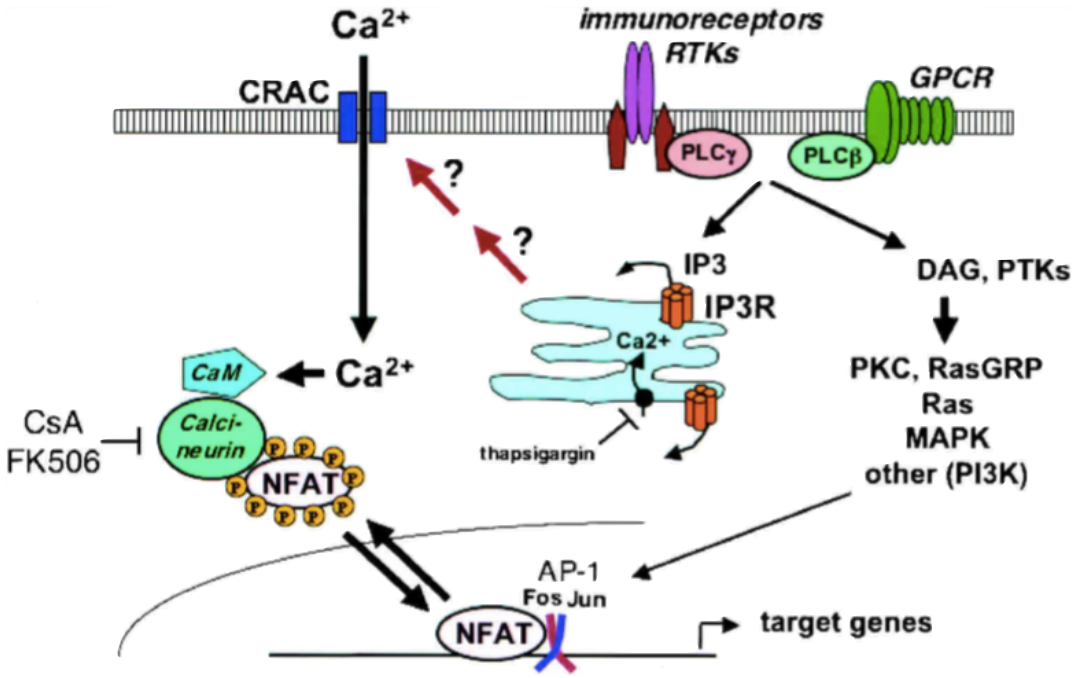

Figure 13: The mechanism of NFAT activation by SOCE. Upon the immunoreceptor activation, the IP_3 activate the IP_3 receptors, releasing the calcium from the ER. This triggers the SOCE mechanism and facilitates Ca^{2+} entry into the cell. The calcium molecules activate the calmodulin (CaM) which transacts the signal to the phosphatase calcineurin. Upon activation, the calcineurin quickly and greatly dephosphorilates NFAT molecules, which can then travel into the nucleus and initiate the gene expression (Hogan et al. 2003).

2.2.2.Experimental Setup

The RBL cells were exclusively used for the NFAT reporter assay. The cells were electroporated with 6 µg of YFP-Orai1 and 12 µg of pNFAT-TA-mRFP DNA and incubated at 37°C with 5% CO_2 atmosphere and humidity of 95% in MEM medium. The cells were measured 24-30 hours after the electroporation. In case of mutants altering the gating of the Orai1 channel by switching it to the partially open or fully open conformation, the RFP production was observed. The cells were measured in a 2 mM Ca^{2+} extracellular medium. The solution contained 2 mM calcium chloride, 140 mM sodium chloride, 5 mM potassium chloride, 1 mM magnesium chloride, 10 mM HEPES and 10 mM glucose with final pH of 7.4. Cells with similar expression levels of YFP-Orai1 were selected to achieve comparable results. The cells were monitored using Axiovert 100 TV microscopy and the fluorescence of the individual cells was observed. The YFP-Orai1 was monitored with excitation of 514 nm for 2000 ms and the RFP was recorded with excitation of 565 nm for 300, 500 and 1000 ms. The threshold to consider the cell as activated was set to 2, 4 and 8 a.u. (arbitrary units) intensity respectively.

For the assay-efficiency experiments, the cells were electroporated with 6 µg of YFP-Orai, 6 µg of CFP-STIM1 and 12 µg of pNFAT-TA-mRFP DNA. The Orai was used in all its homologs (Orai1, Orai2 and Orai3) and the Orai1 E106Q mutant was also measured as a representative of a negative channel activity. The cells were kept in MEM medium and stimulated with 0.1 µM Thapsigargin (TG) prior to the measurement. The RFP intensity was measured 2, 2.5, 3, 3.5, 4 and 4.5 hours after the TG treatment to determine the best time period for the reproducible measurements. The comparability of the cells was measured by its YFP-Orai expression. The RFP was recorded with excitation at 1, 2 and 5 s with the intensity threshold set to 2, 5 and 15 a.u. (arbitrary units) respectively.

2.3.Cell Culture

2.3.1. HEK cells

The HEK293 cells originate from modified human embryonic kidney cells. Those cells are widely accepted as a study model for their easy preparation and a low expression level of endogenous ion channels. The proteins of interest can be easily inserted by transfection using TransFectin™ lipid reagent. This reagent binds to the protein DNA and delivers it into the cells with high effectiveness. The process of transfection consists of mixing the DNA and the reagent in a solution and then applying it directly to the cells. For the proper growth the medium is exchanged after 3.5 hours.

For the patch clamp measurements it is necessary to immobilise the cells on a glass slide. For this purpose the glass slides were treated with a poly-L-lysine solution that creates a thin film for cells to attach. In order to reseed the cells on the coated slides, they were washed with a PBS solution and then treated with a trypsin-EDTA solution for 8-10 minutes to detach. Once the cells were in the solution the trypsin reaction was stopped by adding a DMEM medium and the cells were centrifuged for 5 min at 1000 rpm. The supernatant was then removed and the cell pellet was redesolved in a DMEM medium. Those cells were then applied to the glass slides and measured at least 4 hours later.

2.3.2. RBL cells

The RBL cells are rat basophilic leukaemia cells and are a common model for immunity studies for their similarity to mast cells. The desired proteins are introduced using an electroporation method that uses an electric field to create pores in a cell membrane allowing the protein DNA to flow inside.

Prior to the electroporation, the cells must be detached in order to be transferred as the process takes place in solution. For that purpose the cells were first washed with PBS and treated with a trypsin-EDTA solution for 8-10 minutes. The trypsin reaction was then stopped using a MEM medium and the cells were centrifuged for 5 min at 1000 rpm. The supernatant was discarded and the cell pellet was redesolved in an electroporation buffer. The electroporation buffer contained 15 mM potassium glutamate, 2 mM HEPES, 0.7 mM magnesium diacetate, 0.1 mM EGTA and 4.54 mM glucose with pH 7.4. The protein DNA was then introduced into the solution and the mixture was transferred into the cuvette. The electroporator settings were 200V and 525pF and the pulse was applied. The cell solution was then transferred on glass slides in a MEM media. The medium was exchanged after 3.5 hours and the cells were measured the following day.

2.4.Used Solutions

Extracellular 0 mM Ca^{2+} solution

The solution contained sodium chloride (140mM), potassium chloride (5mM), magnesium chloride (1mM), HEPES (10mM) and glucose (10mM) with pH 7.4.

Extracellular 2 mM Ca^{2+} solution

The solution contained calcium chloride (2mM), sodium chloride (140mM), potassium chloride (5mM), magnesium chloride (1mM), HEPES (10mM) and glucose (10mM) with pH 7.4.

Extracellular 10 mM Ca^{2+} solution

The solution contained calcium chloride (10mM), sodium chloride (140mM), caesium chloride (5mM), magnesium chloride (1mM), HEPES (10mM) and glucose (10mM) with pH 7.4.

Intracellular pipette solution

The solution contained EGTA (20mM), caesium methanesulfonate (145mM), sodium chloride (8mM), magnesium chloride (5mM) and HEPES (10mM) with pH 7.2.

DMEM high glucose medium with sodium pyruvate and L-glutamine (P04-05550)

MEM Eagle medium with EBSS and L-glutamine (P04-08500)

Trypsin EDTA without Ca and Mg (P10-023100)

TransFectin™ Lipid Reagent (BioRad #170-3352)

DPBS without Ca and Mg solution (P04-36500)

Electroporation buffer

The buffer contained potassium glutamate (15mM), HEPES (2mM), magnesium diacetate (0.7mM), EGTA (0.1mM) and glucose (4.54mM) with pH 7.4.

3. Results and Discussion

3.1. NFAT Reporter Assay

3.1.1. Assay efficiency

The activation of the transcription factor NFAT has been well described for Orai1 channels. Initially I intended to evaluate if the other isoforms of Orai1 are also able to induce the NFAT driven gene expression and thus here I evaluate all three isoforms of Orai. Carcinogenic mutations of Orai2 and Orai3 will be measured in the future as a follow-up of this work. The efficiency of the NFAT driven gene expression, named the NFAT reporter assay was evaluated for the Orai channel family, including Orai1, Orai2, Orai3 and the non-permeable Orai1-E106Q mutant.The YFP-tagged Orai isoforms were individually co-expressed with CFP-STIM1 and RFP under control of the NFAT promoter in order to determine the most efficient measurement time for the RFP production. The transfected RBL cells were treated with a 100nM thapsigargin solution to activate SOCE and measured 2, 2.5, 3, 3.5, 4 and 4,5 hours after the stimulation. The cells were always stimulated by thapsigargin 24 hours after the transfection. The obtained results for the RFP production efficiency and the RFP intensity compared for each measurement are shown in figures 14-17. To ensure the comparability of the measured samples, the expression of the YFP-Orai was compared and the results can be seen in figure 18.

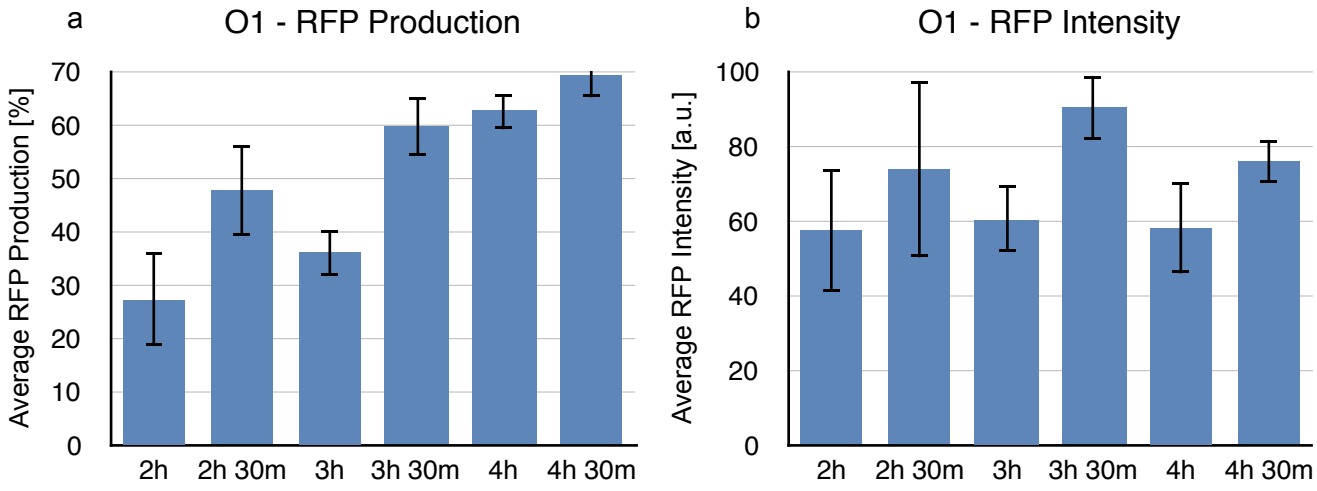

Figure 14: Expression of NFAT driven RFP determined for the respective time for RBL cells co-expressing CFP-STIM1 and YFP-Orai1. (a) The average RFP production indicates the percentage of cells positive for the RFP production. (b) The average RFP intensity at 5s illumination over time showing slight variation with the highest intensity for 3.5h of thapsigargin stimulation. The error bars indicate the standard error of mean in both cases. The number of measured cells was n= 64, 59, 57, 49, 54 and 48 for 2h, 2.5h, 3h, 3.5h, 4h and 4.5h respectively and were collected on 3 separate measurements. The a.u. stands for arbitrary units.

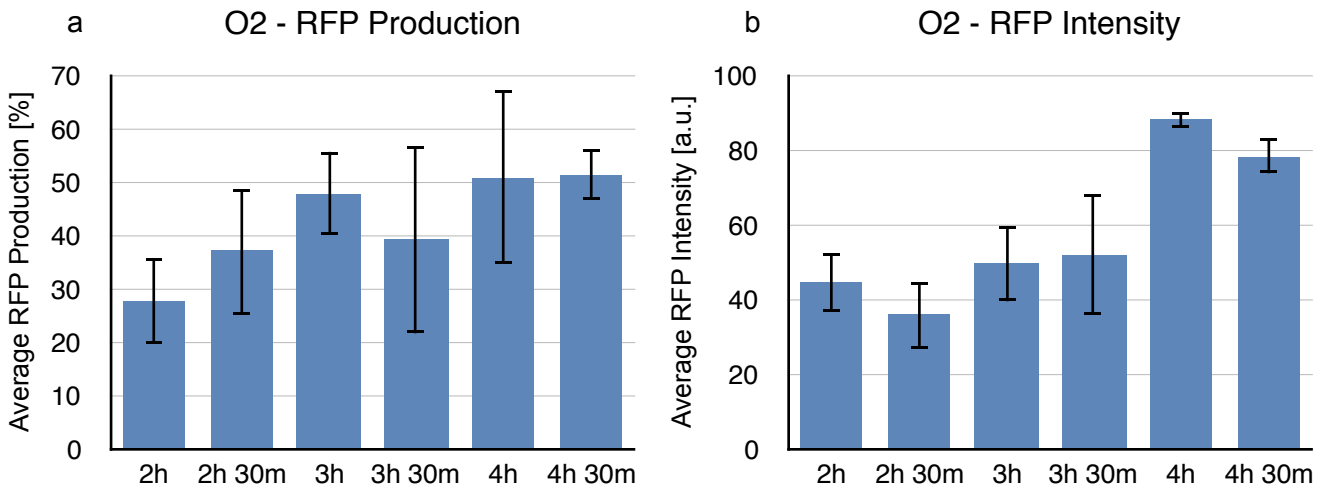

Figure 15: Expression of NFAT driven RFP determined for the respective time for RBL cells co-expressing CFP-STIM1 and YFP-Orai2. (a) The average RFP production indicates the percentage of cells positive for the RFP production. (b) The average RFP intensity at 5s showing generally increasing trend over time. The error bars indicate the standard error of mean in both cases. The number of measured cells was n= 61, 58, 58, 62, 64 and 58 for 2h, 2.5h, 3h, 3.5h, 4h and 4.5h respectively and were collected by 3 separate measurements. The a.u. stands for arbitrary units.

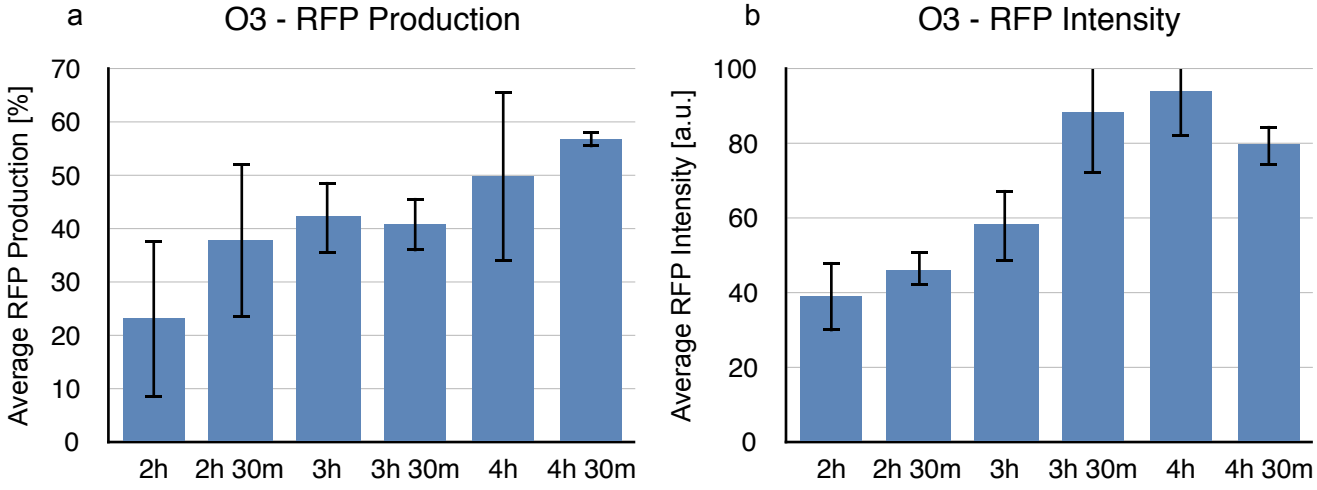

Figure 16: Expression of NFAT driven RFP determined for the respective time for RBL cells co-expressing CFP-STIM1 and YFP-Orai3. (a) The average RFP production indicates the percentage of cells positive for the RFP production. (b) The average RFP intensity at 5s showing generally increasing trend over time with a drop in the last point. The error bars indicate the standard error of mean in both cases. The number of measured cells was n= 49, 46, 54, 47, 45 and 46 for 2h, 2.5h, 3h, 3.5h, 4h and 4.5h respectively and were collected by 3 separate measurements. The a.u. stands for arbitrary units.

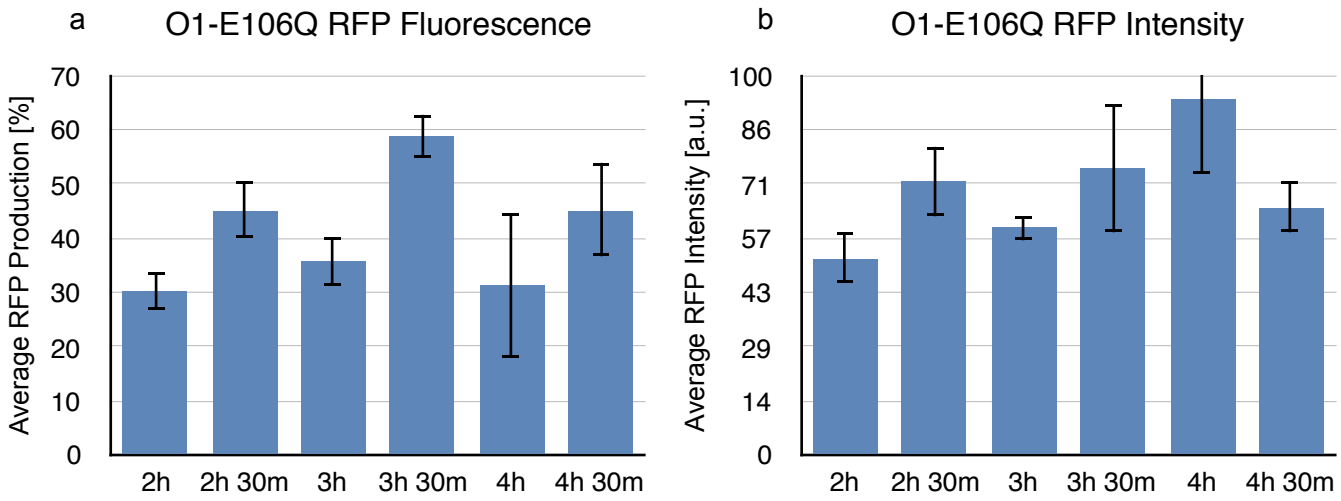

Figure 17: Expression of NFAT driven RFP determined for the respective time for RBL cells co-expressing CFP-STIM1 and YFP-Orai1-E106Q. (a) The average RFP production indicates the percentage of cells positive for the RFP production. (b) The average RFP intensity at 5s illumination over time showing slight variation. The error bars indicate the standard error of mean in both cases. The number of measured cells was n= 67, 61, 68, 62, 66 and 64 for 2h, 2.5h, 3h, 3.5h, 4h and 4.5h respectively and were collected on 3 separate measurements. The a.u. stands for arbitrary units.

From the figures 14-17 can be concluded that the RFP production caused by the CRAC channels stimulated by the thapsigargin was successfully measured with high reproducibility. The expression in Orai2 and Orai3 is slightly lower compared to the Orai1 and the mutant. This might be due to a reduced calcium influx into the RBL cells, in line with previous results (Lis et al. 2006). The general trend shows a peak of RFP expression between 3.5 and 4 hours with possible decrease at 4.5h. This locates the ideal measurement time in this time period as later the cells might already undergo apoptosis due to prolonged treatment with thapsigargin. It is of note that over-expression of the pore mutant Orai1-E106Q resulted in a robust NFAT driven gene expression. These results suggest that the endogenous CRAC channels are not sufficiently inhibited. A possible reason is that the endogenous CRAC channels are formed without including any dominant negative Orai1-E106Q subunits. Hence, the remaining endogenous CRAC channels are sufficient to express RFP upon the NFAT stimulation. The YFP-Orai expression for each measurement is showed in figure 18 showing similar levels and thus allowing to compare the results.

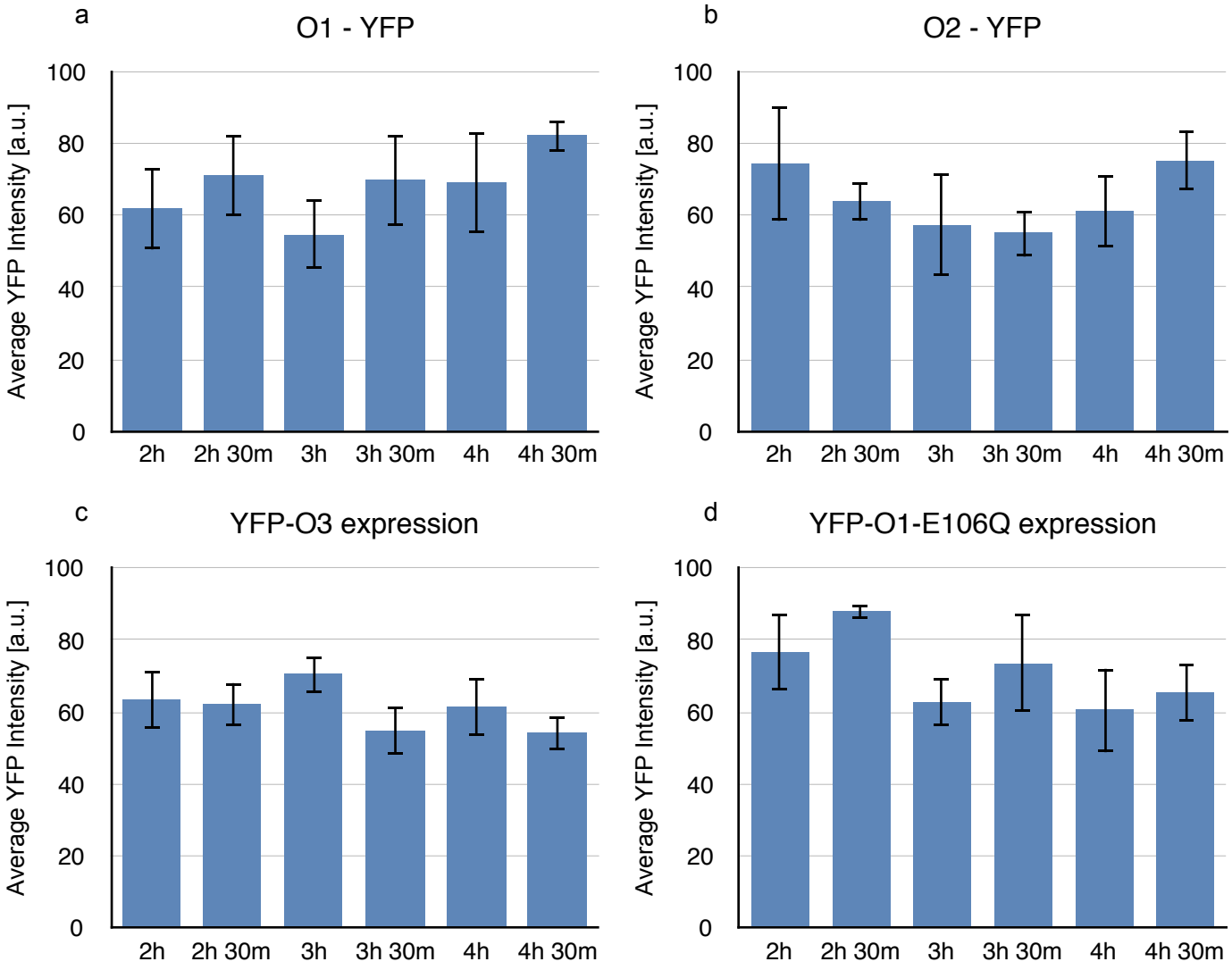

Figure 18: The comparison of levels of the expression by measurement of the YFP-Orai intensities for (a) YFP-Orai1, (b) YFP-Orai2, (c) YFP-Orai3 and (d) YFP-Orai1-E106Q.

3.1.2. Carcinogenic mutants

The cBioPortal (http://www.cbioportal.org) was screened for the Orai1 mutations discovered in various cancer-related studies. As a result, I created a list of 24 point mutations which were evaluated for the consensus of the original amino acid among 103 eukaryotic organisms following a hypothesis that a mutation in more conserved amino acids is more likely to have a severe effect on the protein. The threshold was set to 45% and the mutations that were conserved above the threshold were selected for the experiment. In addition to 14 mutations, coming from the cancer studies, I added 3 other mutants previously described to modify Orai1 gating. Wild type Orai1 was used as a control for the experiment, representing the closed conformation in the absence of the store depletion and STIM1 expression. The selected mutations can be found in a Table 1 with their source cancer study and consensus. The visualisation of the mutants of an Orai1 subunit is shown in figure 19.

Table 1: Orai1 mutants selected for the experiment derived form large-scale cancer databases

cBioPortal	Cancer study	Consensus [%]
S90G	Colorectal	75
M104V	Leukaemia	90
I121T	NCI-60	80
A137V	Colorectal	98
M139V	Stomach	99
S159L	Uterine	59
R170C	Bladder	94
A177D	NCI-60	88
G183D	Glioblastoma	99
T230I	Melanoma	48
G247S	Head and neck	63
V255I	Uterine	69
R268Q	Uterine	64
N274K	Melanoma	48
Additional mutations		
V102A	Hydrophobic gate with close proximity to selectivity filter E106	
H134A	Suggested to alter gating	
L138F	Linked to tubular aggregate myopathy	

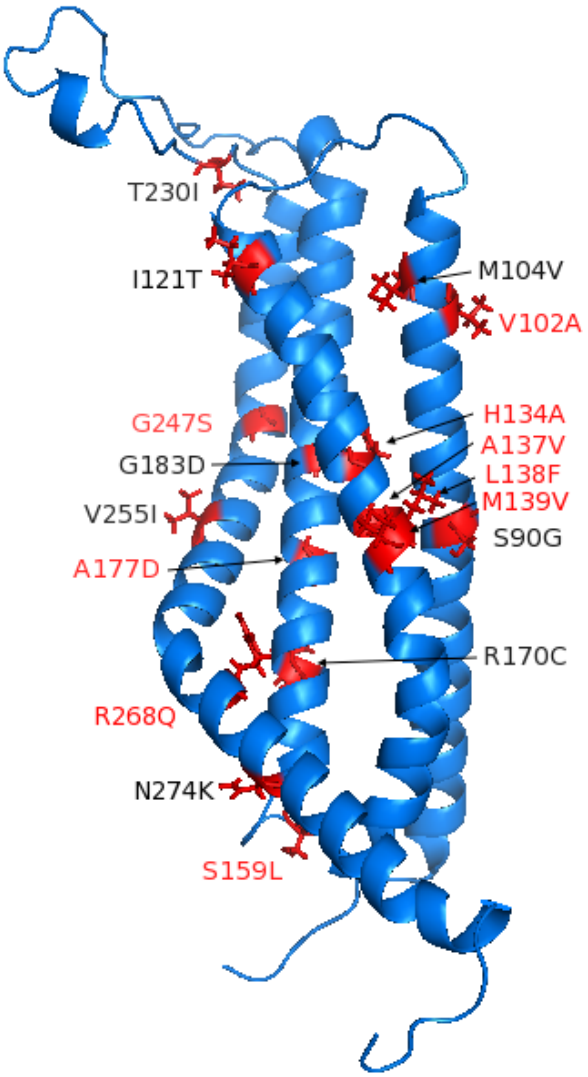

Figure 19: The location of the investigated mutants shown on a subunit of an Orai1 channel. The mutations that significantly alter the channel gating are highlighted in red. All mutants were derived from human cancer patients, except for L138F from a patient with myopathy, V102A, a constitutively active mutant (McNally et al. 2012) and H134A (unpublished results, Frischauf et al.).

Those mutations created a pool of 17 samples that were investigated using the NFAT reporter assay and statistically compared to the wild type Orai1 data using the students t-test. The respective Orai1 mutants were co-expressed with the NFAT reporter in RBL cells and monitored for RFP production after 24 hours in a Ca^{2+} containing medium. The mutation Orai1-G183D showed mis-localisation as the fluorescence was observed in the cytosol instead of the plasma membrane and thus was not included in the NFAT reporter assay measurements. All the other mutants were localised in the plasma membrane. The data from the NFAT reporter assay are shown in figure 20. The number of RFP expressing cells of cancer mutants were compared with those of wild type Orai1 for significant difference. The representative image of the measured cells for the wild type Orai1, O1-A137V mutant and O1-G247S mutant are shown in figure 21. The comparison of the YFP-Orai1 expression level over the samples is shown in figure 22.

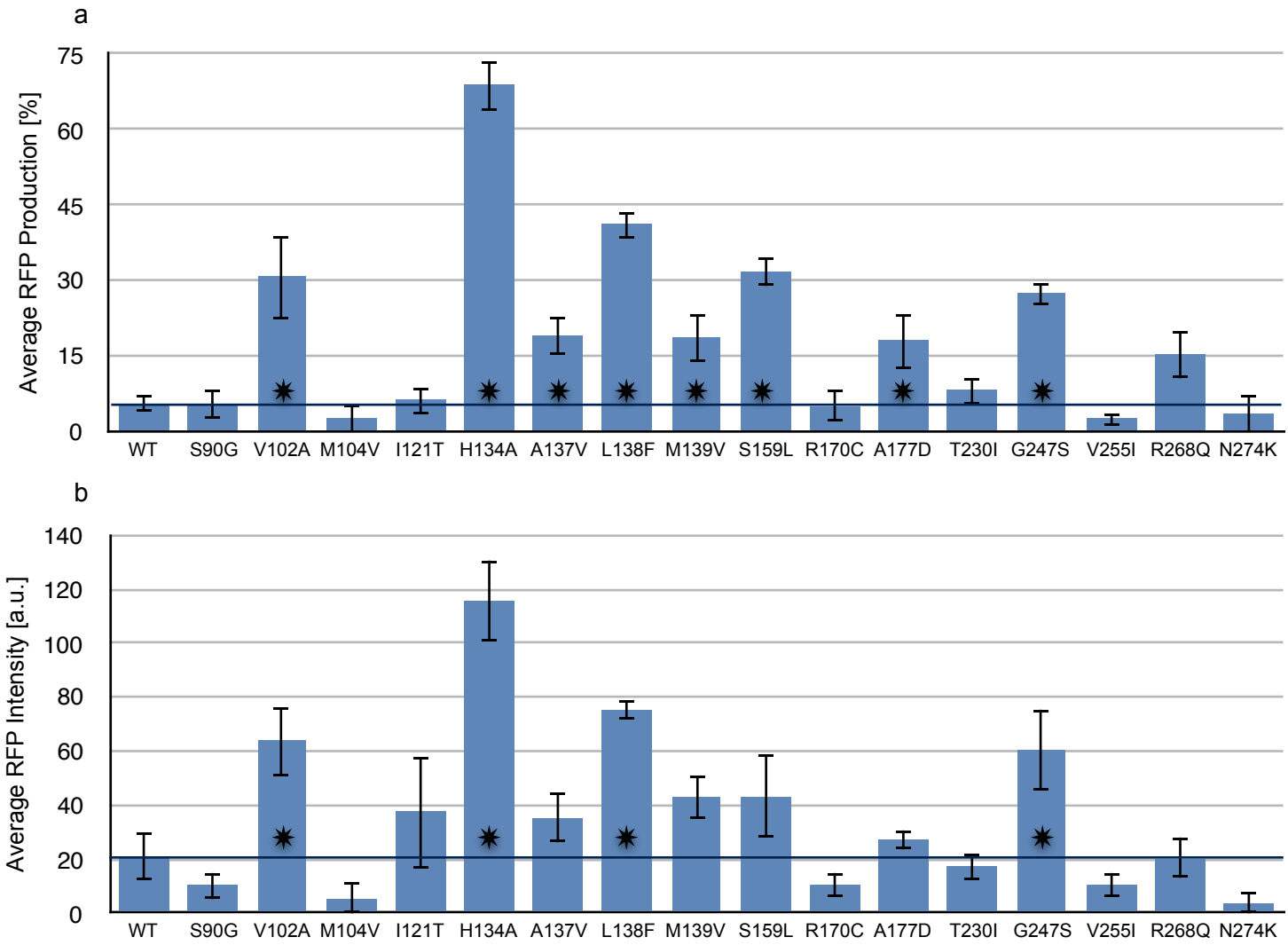

Figure 20: The average NFAT driven RFP production for the selected Orai1 mutants and wild type (WT). (a) The average RFP production indicates the percentage of cells positive for the RFP production. (b) The average RFP Intensity at 1s excitation time for the selected Orai1 mutants and the wild type. The standard error of mean is represented by the error bars in both cases. The value for the WT measurement is depicted as a baseline. The asterisk indicates the results significantly different from the WT ($p<0.05$). Each sample was measured 4-5 days with the final number of cells n= 192, 148, 91, 118, 180, 139, 208, 143, 120, 87, 98, 143, 155, 98, 167, 80 and 87 for WT, S90G, V102A, M104V, I121T, H134A, A137V, L138F, M139V, S159L, R170C, A177D, T230I, G247S, V255I, R268Q and N274K respectively.

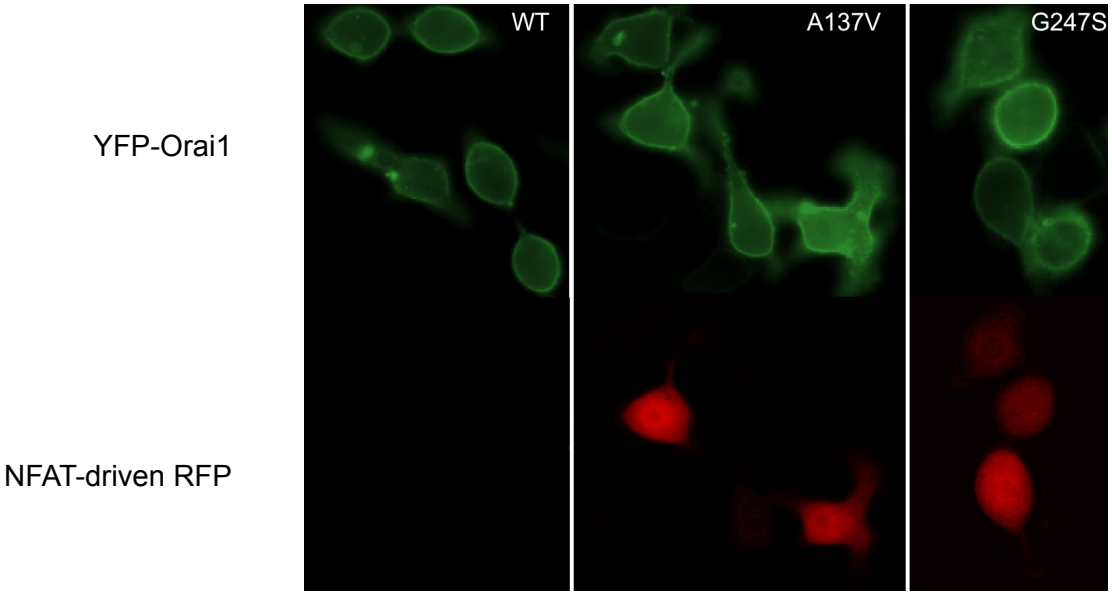

Figure 21: Representative images of the measured cells. The YFP-tagged Orai1 with membrane localization (green) and the RFP produced by the NFAT reporter (red).

Figure 22: The YFP-Orai1 mutations expression levels.

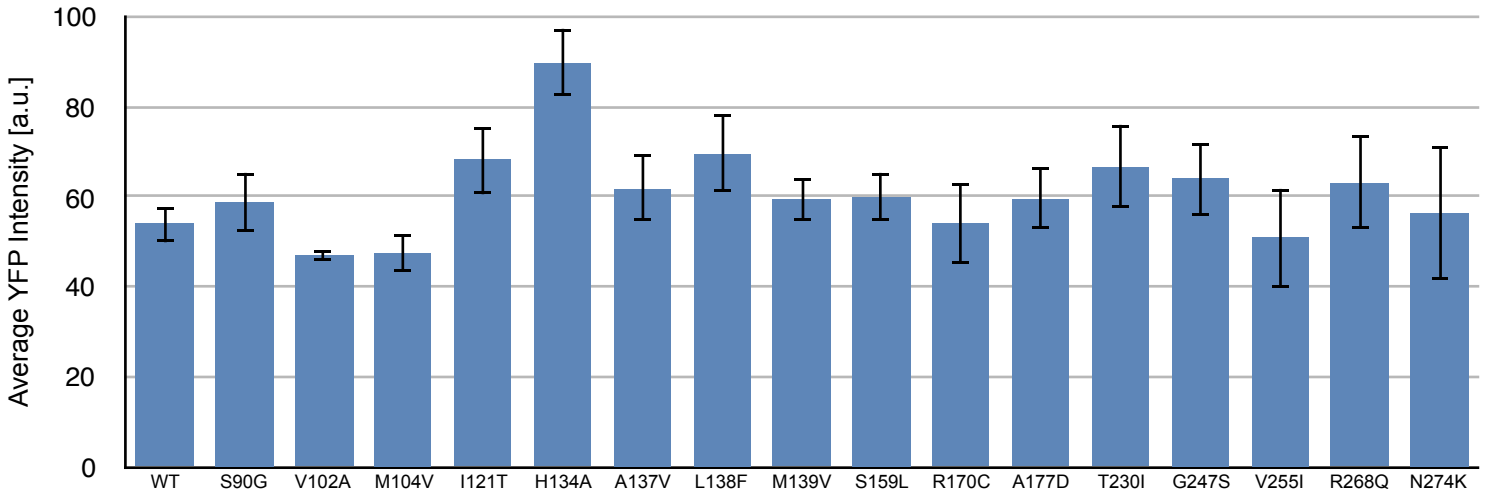

From the final data (figure 20) I obtained 8 hits, which show significantly elevated RFP production without cell stimulation, suggesting that those mutants modify gating of the Orai1 protein by switching it to partially or fully opened conformation and trigger the NFAT driven gene expression. The middle region of the second Orai1 TM helix (residues 134-139) shows high signals with a peak at position H134A (see fig 19). This suggests the importance of this region for gating of the channel. Residues in this region are most likely responsible for switching the channel into its open conformation. The RFP intensity levels correspond to the production levels. The expression levels of YFP-O1 mutants are generally in similar range allowing us to compare the samples (figure 22).

3.1.3. Orai1 H134 point mutations

From the previous data I obtained the strongest signal for mutant H134A. To further investigate its importance I performed the following experiments with constructs containing various point mutations in position 134. The H134A was used as a reference for the maximal signal and wild type Orai1 was used as a negative control. The NFAT reporter assay was performed and the data can be seen in figure 23. The YFP-Orai1 expression level comparison is shown in figure 24.

Figure 23: The average NFAT driven RFP production for the selected Orai1-H134 mutants and wild

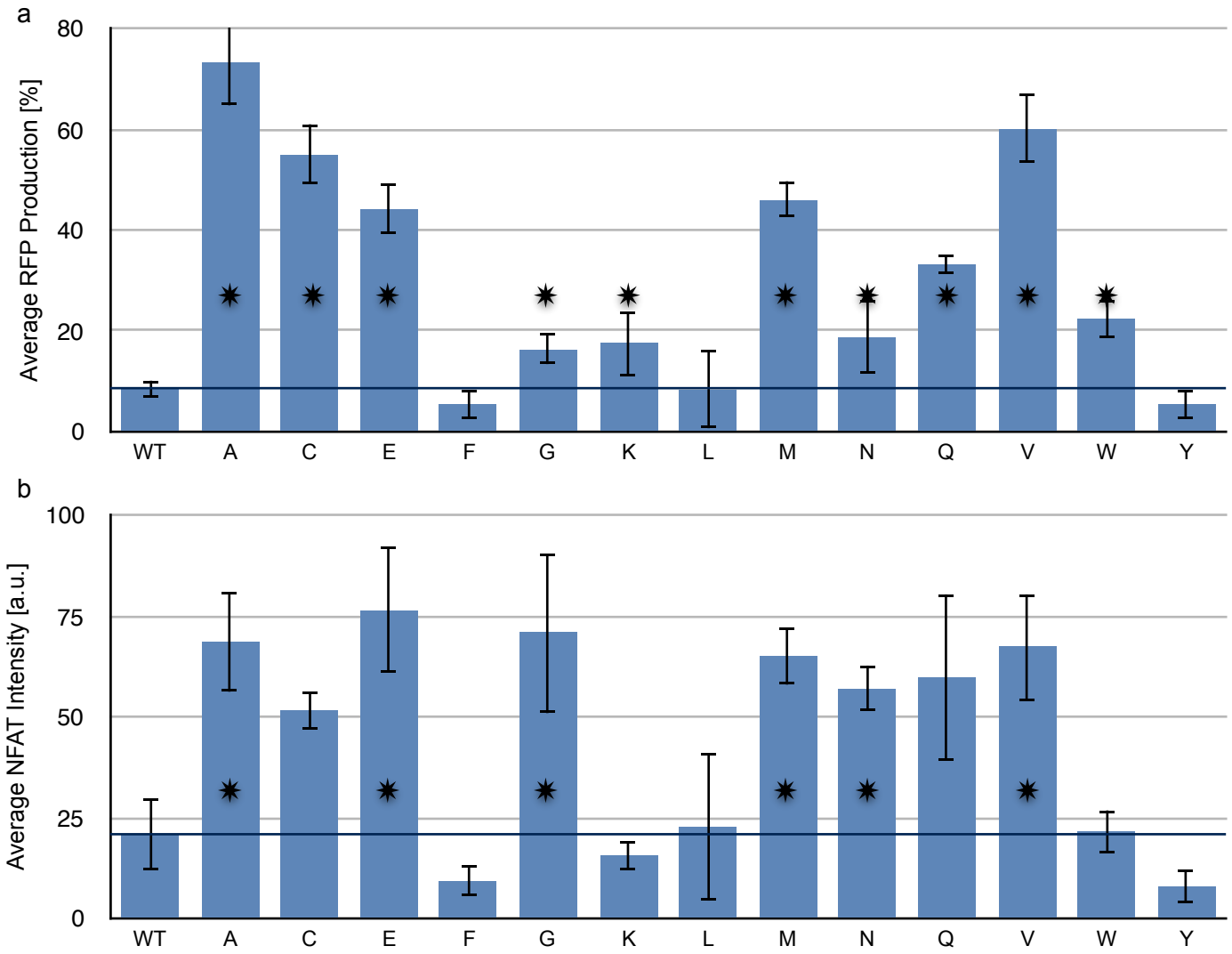

type (WT). (a)The point mutation is represented by the amino acid letter placed in position 134 replacing the histidine. The average RFP production indicates the percentage of cells positive for the RFP production. (b) The average RFP intensity at 1s excitation time for selected Orai1-H134 mutants and wild type. The value from WT measurement is depicted as a baseline. The standard error of mean is represented by error bars. Each sample was measured over 3-4 days with final number of cells n= 76, 49, 58, 72, 75, 80, 79, 65, 72, 84, 53, 52 and 48 for H134A, H134C, H134E, H134F, H134G, H134K, H134L, H134M, H134N, H134Q, H134V, H134W and H134Y respectively.

Figure 24: The YFP-Orai1-H134 mutants expression levels.

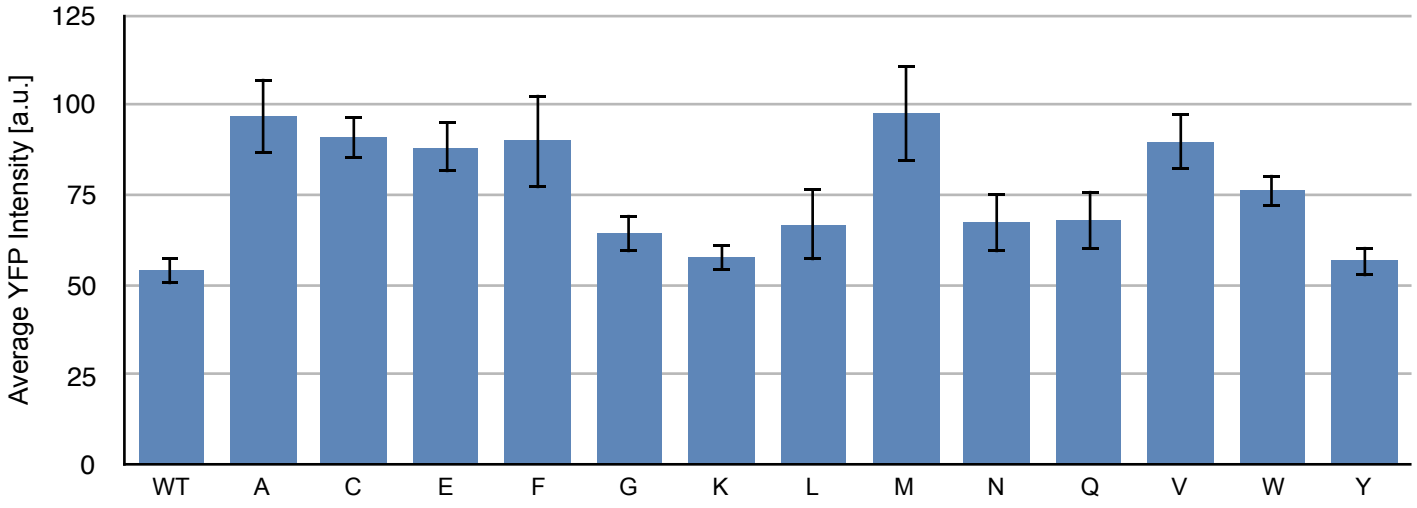

Those experiments underline the importance of the O1-H134A mutant as no other residue showed higher signal. Other residues in this position can be roughly grouped by their effect on the channel and their size. Generally spatially small residues (C, E, M, V) show a switch to the partially open conformation. The Orai1-H134G, H134N and HN13Q showed relatively low amount of the RFP expressing cells, however the active ones resulted in a similar high RFP intensity as that of Orai1-H134A. On the other hand, spatially large residues (F, L, Y) seem to block the channel opening and exhibit signals smaller or comparable to the wild type Orai1. The Intensity of the RFP signals seems roughly comparable to the RFP production but with higher variation through the mutations. The YFP-O1 signals for wild type are generally low but amongst the H134 mutations the levels are comparable.

.

3.1.4.Orai1 G183 point mutations

The initial screening also indicated the Orai1-G183D mutation. This mutation comes from a glioblastoma cancer study and the glycine in position 183 is conserved up to 99% over eukaryotic species. The fluorescence measurements discovered that the mutation causes the delocalisation of the Orai1 into the cytosol. To further investigate this effect, G183 was substituted with different amino acids to gain more insight into the conditions of the protein PM localisation. The comparison of the WT Orai1 and other Orai1-G183 mutants can be seen in figure 25.

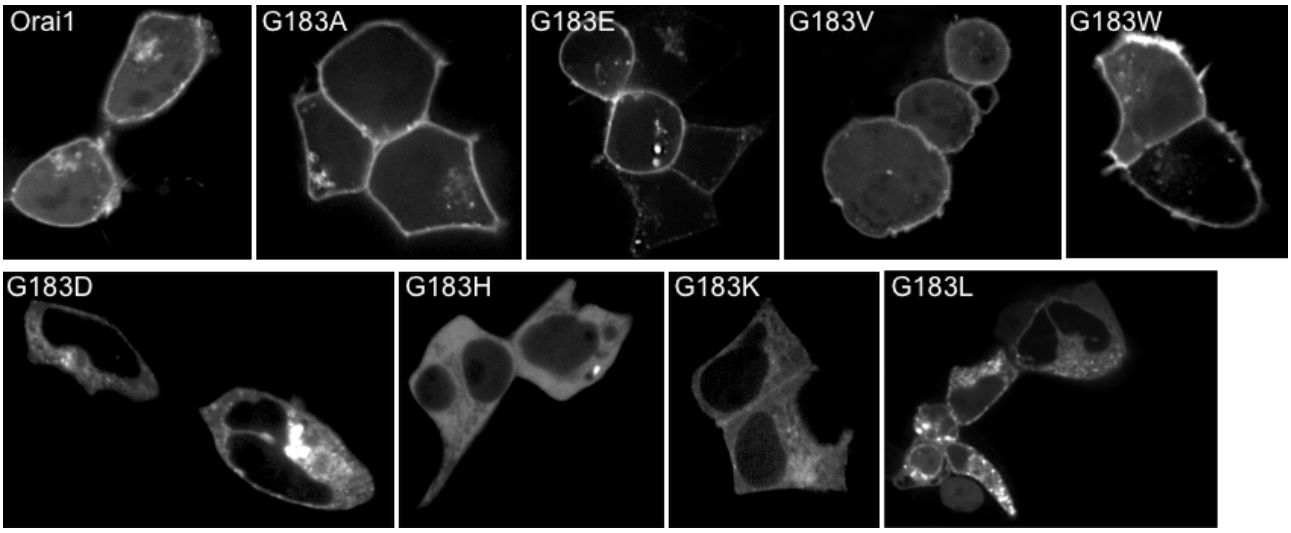

Figure 25: The fluorescence images of YFP-Orai1 and different YO1-G183 mutants with focus on localisation.

The Orai1-G138 experiments included 6 different mutations which were investigated in the means of localisation of the protein into the membrane. The original O1-G183D was delocalised into the cytosol as shown in figure 24. This might be due to steric reasons as the aspartic acid is much larger than the glycine, or the additional charge changing the polarity of the region. Three of the selected mutants proved to maintain the plasma membrane localisation as the wild type. The O1-G183A with a small side chain of alanine probably doesn't produce much of spatial hindrance inside the Orai1 structure, still allowing the PM localisation. Surprisingly the O1-G183E with glutamic acid allowed the plasma membrane localisation despite its similarity to the aspartic acid. The O1-G183W might have a stabilising effect on the surrounding residues, allowing the PM localisation despite its relatively large size. The other three studied mutations introduced a state similar to the O1-G183D with delocalisation into the cytosol. The O1-G183H and O1-G183K with positively charged side chains might cause the destabilisation of the structure and thus causing the delocalisation. The mutations were not tested for channel functionality.

3.2.Patch Clamp Results

To further investigate the modifications caused to the channel by different carcinogenic mutations, patch clamp experiments were conducted. Some of the mutants which showed significant effect on the Orai1 channel gating were measured with the whole cell patch clamp technique. The bath solution contained 10mM Ca^{2+} while the cytosolic Ca^{2+} was buffered with 20mM EGTA in the pipette solution. Voltage ramps were applied every 5s and currents were recorded at -74mV. The results of these time course experiments can be seen in figure 26.

The only mutant that showed the expected partially constitutive activity was O1-A137V. The currents of the other samples were not large enough to prove a constitutive activity by the patch clamp technique.This suggests that those mutants produce only a small constitutive Ca^{2+} influx which may be able to activate the NFAT driven gene expression while avoiding overload of Ca^{2+} into the cell to preserve its viability.

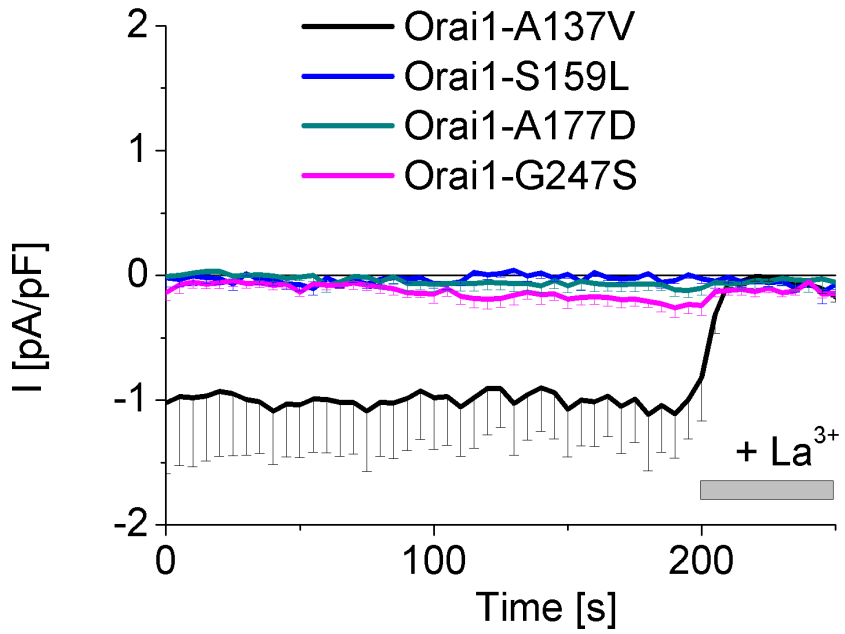

Figure 26: The whole-cell patch clamp measurements showing the time course currents of the HEK cells expressing different Orai1 mutants in presence of 10mM extracellular calcium. Only the O1-A137V shows measurable signals, all the other mutations fail to produce currents. For the leak current subtraction, the channels were blocked by La^{3+} at the end of the measurement.

The Orai1-A137V was further investigated in the experiments where it was co-expressed with STIM1 protein. In this case the channel showed partially constitutive currents which were further increased upon store depletion to the fully activated form. The results of those measurements can be seen in figure 27. The selectivity of the channel was examined and the results for Orai1-A137V with or without STIM1 are shown in figure 28.

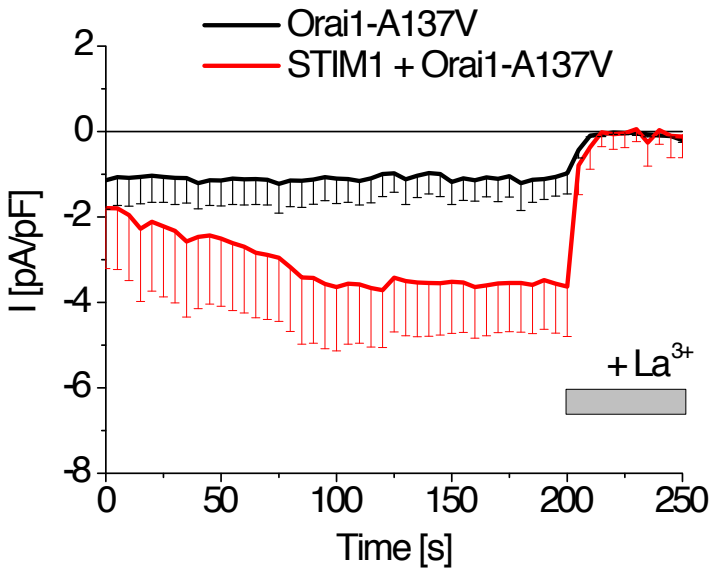

Figure 27: The whole-cell patch clamp measurements showing the time course currents in HEK cells expressing Orai1-A137V without (black) or with (red) STIM1 in a bath solution containing 10 mM Ca^{2+}. Current activation by the endoplasmic reticulum store depletion was mediated by 20 mM EGTA in the patch pipette. For the leak current subtraction, the channels were blocked by La^{3+} at the end of the measurement.

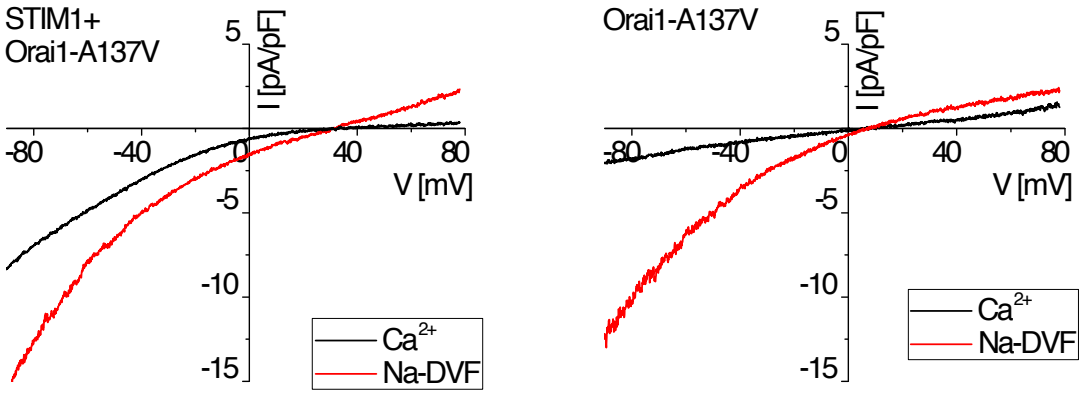

Figure 28: Representative current-voltage relationship of Orai1-A137V with and without STIM1. Co-expression of Orai1-A137V and STIM1 showed a signals characteristic for WT O1 with STIM1. The shift in the signals in the right image shows a reduced Ca^{2+} selectivity of the Orai1-A137V without STIM1.

From those experiments it is visible that the O1-A137V mutation is directly affecting gating of the Orai1 channel and it selectivity. The cells with this mutation exhibit a disrupted calcium signalling and altered gene regulation. The location of this mutant in the Orai structure is underlining the importance of this region for the gating of the channel.

4. Conclusion

The role of Ca^{2+} signaling in cancer development is an emerging topic. Specifically, the store-operated Ca^{2+} channel components STIM1 and Orai1 have been shown to contribute to critical steps that lead to malignant cancer cells (Hoth 2015). However, it still needs to be determined if Ca^{2+} signaling proteins are driver genes for general cancer cell development. This issue becomes even more complex as the STIM/Orai channel family contributes of two STIM and three Orai isoforms. Moreover, other Ca^{2+} selective channels including TRP channels or Ca^{2+} selective channels in the ER or mitochondria might play a cooperative function.

In my thesis I have analyzed Orai1 mutants, determined from large genome wide cancer studies that revealed multiple possible candidates. Those mutants create a number of possible sites for a modification of structure and function of the Orai1 protein. To quantitatively evaluate the effect of these Orai1 mutants, the fluorescence intensity of red fluorescent protein under control of an NFAT promoter was determined. From the original pool of 17 investigated mutations, 8 showed to be significantly more effective to induce activation of NFAT driven genes than the wild type protein. Among these active Orai1 mutants are V102A, H134A, A137V, L138F, M139V, S159L, A177D, G247S and R268Q.

It is of note that the middle region of a second trans-membrane helix seems to be of a crucial importance including two cancer mutants as well as L138F, which was reported to cause tubular aggregate myopathy in patients. The neighbouring cancer mutations A137V and M139V were associated with a colorectal and stomach cancer respectively. In addition, I investigated nearby H134 mutations that switched the Orai1 protein to partially or fully open conformation. The highest results were obtained for the Orai1-H134A mutation that was previously investigated in our laboratory and was suggested to alter the gating of the protein. The Orai1-H134A mutant resulted in a constitutive channel activity, even in the absence of STIM1 and store-depletion.

Instead, only the Orai1-A137V resulted in visible constitutive channel activity while the other here determined cancer mutants may have Ca^{2+} signals below the detection limit of the patch-clamp technique. Clearly the NFAT reporter assay is a very sensitive method to determine small constitutive Ca^{2+} signals as it senses the calcium-driven NFAT gene expression over 24 hours. Currents of the Orai1-A137V showed a reversal potential around 0mV in both a 10mM Ca^{2+} containing solution and a Na^{+} divalent free solution. Instead, for STIM1 and Orai1-A137V currents the reversal potential shifted rightwards to more Ca^{2+} and Na^{+} selective currents. This is in line with a previous report for the pore mutant Orai1-V102A that showed a similar increase in Ca^{2+} selectivity by STIM1 (McNally et al, 2012). Further studies will need to evaluate the cancer mutants by Ca^{2+} imaging techniques that might be more sensitive to small increases in cytosolic Ca^{2+} than electrophysiological recordings. Ongoing experiments from a biochemical cysteine scanning

suggest that all those residues alter the gating of the protein and allow calcium influx independent of the store depletion. Those findings support the hypothesis that this region acts as a pivot point for the channel opening.

The increased Ca^{2+} levels might be beneficial to trigger the carcinogenic genes in the cells and thus increase the probability of the cancer onset. This explains why many of the cancer-related mutations showed the increased channel opening. The thapsigargin experiments inducing a long-term Ca^{2+} influx resulted in the apoptosis of the cells, showing that extensive high calcium signals are not beneficial for the cells. Thus it is unlikely that the oncogenic mutations would result in extreme Ca^{2+} signals and NFAT gene regulation as the Orai1-H134A mutant. This is supported by my patch-clamp results that showed mostly small or non-recordable constitutive signals for those mutations.

The Orai1-H134 was further investigated for various mutations with the highest signal for an original alanine mutation. The resulting effect of each mutation often seems to be directly linked to the properties of the amino acid placed in the position. Small residues as cysteine, valine and methionine switched the channel to the partially open conformation. On the contrary the residues with a large side chain showed the values lower or comparable to the wild type Orai1, suggesting that the channel might be constitutively closed due to the steric hindrance. In case of arginine mutation the channel lost its ability to localise on a plasma membrane suggesting that it disrupts the ability of protein assembly.

A mutation Orai1-G183D was also included in the initial experiments for its connection to the glioblastoma multiforme. The introduction of the mutated Orai1 caused the disrupted localisation of the protein into the cytoplasm of the cell. The mutation seems to affect the protein assembly either due to the steric reasons or the additional negative charge of the aspartic acid. For further insight we inserted other amino acids into this position. Surprisingly glutamic acid restored the membrane localisation as well as a large tryptophan. The membrane localisation was also restored by spatially small alanine. However, positively charged histidine and leucine showed delocalisation as well as lysine. In the future, the membrane-localised mutants should be also studied in the terms of activity to determine if the protein function is conserved.

This study reveal the importance of the middle of a second TM helix and propose its function as a pivot point for the channel gating. The future investigation of these oncogenic mutants should be done in their cell line of origin to follow their effect on the cancer proliferation, migration and invasion.

Literature

Berridge, Michael J, Martin D Bootman, and H Llewelyn Roderick. “Calcium Signalling: Dynamics, Homeostasis and Remodelling.” Nature reviews. Molecular cell biology 4.7 (2003): 517–529.

Bohm, Johann et al. “Constitutive Activation of the Calcium Sensor STIM1 Causes Tubular-Aggregate Myopathy.” American journal of human genetics 92.2 (2013): 271–278.

Calloway, Nathaniel et al. “Molecular Clustering of STIM1 with Orai1 / CRACM1 at the Plasma Membrane Depends Dynamically on Depletion of Ca 2 ⁒ Stores and on Electrostatic Interactions.” 20 (2009): 389–399.

Catterall, W. A. (2000). "Structure and regulation of voltage-gated Ca2+ channels." Annu Rev Cell Dev Biol 16 (2000): 521-555.

Chen, Yih-Fung et al. “Calcium Store Sensor Stromal-Interaction Molecule 1-Dependent Signaling Plays an Important Role in Cervical Cancer Growth, Migration, and Angiogenesis.” Proceedings of the National Academy of Sciences of the United States of America 108.37 (2011): 15225–15230.

Clapham, David E. “Calcium Signaling.” Cell 131.6 (2007): 1047–1058.

Collins, Sean R, and Tobias Meyer. “Evolutionary Origins of STIM1 and STIM2 within Ancient Ca2+ Signaling Systems.” Trends in cell biology 21.4 (2011): 202–211.

Derler, Isabella et al. “A Ca2(+)release-Activated Ca2(+) (CRAC) Modulatory Domain (CMD) within STIM1 Mediates Fast Ca2(+)-Dependent Inactivation of ORAI1 Channels.” The Journal of biological chemistry 284.37 (2009): 24933–24938.

Endo, Y et al. “Dominant Mutations in ORAI1 Cause Tubular Aggregate Myopathy with Hypocalcemia via Constitutive Activation of Store-Operated Ca2+ Channels.” Hum Mol Genet 24.3 (2015): 637–648.

Faouzi, Malika et al. “ORAI3 Silencing Alters Cell Proliferation and Cell Cycle Progression via c-Myc Pathway in Breast Cancer Cells.” Biochimica et biophysica acta 1833.3 (2013): 752–760.

Fedida-Metula, Shlomit et al. “Lipid Rafts Couple Store-Operated Ca2+ Entry to Constitutive Activation of PKB/Akt in a Ca2+/calmodulin-, Src- and PP2A-Mediated Pathway and Promote Melanoma Tumor Growth.” Carcinogenesis 33.4 (2012): 740–750.

Feng, Mingye et al. “Store-Independent Activation of Orai1 by SPCA2 in Mammary Tumors.” Cell 143.1 (2010): 84–98.

Feske, Stefan et al. “A Mutation in Orai1 Causes Immune Deficiency by Abrogating CRAC Channel Function.” Nature 441.7090 (2006): 179–185.

Feske, Stefan et al. “A Mutation in Orai1 Causes Immune Deficiency by Abrogating CRAC Channel Function.” Nature 441.7090 (2006): 179–185.

Feske, Stefan. “Calcium Signalling in Lymphocyte Activation and Disease.” Nature reviews. Immunology 7.9 (2007): 690–702.

Feske, Stefan. “ORAI1 and STIM1 Deficiency in Human and Mice: Roles of Store-Operated Ca2+ Entry in the Immune System and Beyond.” Immunological reviews 231.1 (2009): 189–209.

Flourakis, M et al. “Orai1 Contributes to the Establishment of an Apoptosis-Resistant Phenotype in Prostate Cancer Cells.” Cell death & disease 1 (2010): e75.

Fracchia, Kelley M, Christine Y Pai, and Craig M Walsh. “Modulation of T Cell Metabolism and Function through Calcium Signaling.” Frontiers in immunology 4.10 (2013): 324.

Frischauf, Irene et al. “A Calcium-Accumulating Region , CAR , in the Channel Orai1 Enhances Ca2+ Permeation and SOCE-Induced Gene Transcription.” 8.408 (2015): 1–13.

Hanahan, D, and R A Weinberg. “The Hallmarks of Cancer.” Cell 100.1 (2000): 57–70.

Hilgemann, D W, S Feng, and C Nasuhoglu. “The Complex and Intriguing Lives of PIP2 with Ion Channels and Transporters.” Science’s STKE : signal transduction knowledge environment 2001.111 (2001): re19.

Hogan, Patrick G, Richard S Lewis, and Anjana Rao. “Molecular Basis of Calcium Signaling in Lymphocytes: STIM and ORAI.” Annual review of immunology 28 (2010): 491–533.

Hoth, M, and R Penner. “Calcium Release-Activated Calcium Current in Rat Mast Cells.” The Journal of physiology 465 (1993): 359–386.

Hoth, Markus. “CRAC Channels, Calcium, and Cancer in Light of the Driver and Passenger Concept.” Biochimica et Biophysica Acta - Molecular Cell Research (2015): 1–10.

Hou, Xiaowei et al. “Crystal Structure of the Calcium Release-Activated Calcium Channel Orai.” Science (New York, N.Y.) 338.6112 (2012): 1308–1313.

Isom, L L, K S De Jongh, and W A Catterall. “Auxiliary Subunits of Voltage-Gated Ion Channels.” Neuron 12.6 (1994): 1183–1194.

Kotturi, Maya F et al. “Identification and Functional Characterization of Voltage-Dependent Calcium Channels in T Lymphocytes.” The Journal of biological chemistry 278.47 (2003): 46949–46960.

Kotturi, Maya F, and Wilfred A Jefferies. “Molecular Characterization of L-Type Calcium Channel Splice Variants Expressed in Human T Lymphocytes.” Molecular immunology 42.12 (2005): 1461–1474.

Lacruz, Rodrigo S, and Stefan Feske. “Diseases Caused by Mutations in ORAI1 and STIM1.” Annals of the New York Academy of Sciences 1356 (2015): 45–79.

Lewis, R S. “Calcium Signaling Mechanisms in T Lymphocytes.” Annual review of immunology 19 (2001): 497–521.

Liu, Huiling et al. “Calcium Entry via ORAI1 Regulates Glioblastoma Cell Proliferation and Apoptosis.” Experimental and Molecular Pathology 91.3 (2011): 753–760.

Luik, Riina M et al. “The Elementary Unit of Store-Operated Ca2+ Entry: Local Activation of CRAC Channels by STIM1 at ER-Plasma Membrane Junctions.” The Journal of cell biology 174.6 (2006): 815–825.

Lyfenko, Alla D, and Robert T Dirksen. “Differential Dependence of Store-Operated and Excitation-Coupled Ca2+ Entry in Skeletal Muscle on STIM1 and Orai1.” The Journal of physiology 586.20 (2008): 4815–4824.

Maus, Mate et al. “Missense Mutation in Immunodeficient Patients Shows the Multifunctional Roles of Coiled-Coil Domain 3 (CC3) in STIM1 Activation.” Proceedings of the National Academy of Sciences of the United States of America 112.19 (2015): 6206–6211.

McAndrew, Damara et al. “ORAI1-Mediated Calcium Influx in Lactation and in Breast Cancer.” Molecular cancer therapeutics 10.3 (2011): 448–460.

McNally, Beth A et al. “Gated Regulation of CRAC Channel Ion Selectivity by STIM1.” Nature 482.7384 (2012): 241–245.

Misceo, Doriana et al. “A Dominant STIM1 Mutation Causes Stormorken Syndrome.” Human mutation 35.5 (2014): 556–564.

Monteith, Gregory R et al. “Calcium and Cancer: Targeting Ca2+ Transport.” Nature reviews. Cancer 7.7 (2007): 519–530.

Muik, Martin et al. “A Cytosolic Homomerization and a Modulatory Domain within STIM1 C Terminus Determine Coupling to ORAI1 Channels.” The Journal of biological chemistry 284.13 (2009): 8421–8426.

Muik, Martin et al. “Ca2+ Release-Activated Ca2+ (CRAC) Current, Structure, and Function.” Cellular and Molecular Life Sciences 69.24 (2012): 4163–4176.

Muik, Martin et al. “Dynamic Coupling of the Putative Coiled-Coil Domain of ORAI1 with STIM1 Mediates ORAI1 Channel Activation.” The Journal of biological chemistry 283.12 (2008): 8014–8022.

Muik, Martin et al. “STIM1 Couples to ORAI1 via an Intramolecular Transition into an Extended Conformation.” The EMBO journal 30.9 (2011): 1678–1689.

Nakamura, Lea et al. “Platelet Secretion Defect in a Patient with Stromal Interaction Molecule 1 Deficiency.” Blood Nov. 2013: 3696–3698.

Navarro-borelly, Laura et al. “STIM1 – Orai1 Interactions and Orai1 Conformational Changes Revealed by Live-Cell FRET Microscopy.” 22 (2008): 5383–5401.

Nesin, Vasyl et al. “Activating Mutations in STIM1 and ORAI1 Cause Overlapping Syndromes of Tubular Myopathy and Congenital Miosis.” Proceedings of the National Academy of Sciences of the United States of America 111.11 (2014): 4197–4202.

Nowycky, Martha C, and Andrew P Thomas. “Intracellular Calcium Signaling.” Journal of cell science 115.Pt 19 (2002): 3715–3716.

Oh-hora, Masatsugu, and Anjana Rao. “Calcium Signaling in Lymphocytes.” Current opinion in immunology 20.3 (2008): 250–258.

Parekh, Anant B. “Store-Operated CRAC Channels: Function in Health and Disease.” Nature Reviews Drug Discovery 9.5 (2010): 399–410.

Park, Chan Young et al. “STIM1 Clusters and Activates CRAC Channels via Direct Binding of a Cytosolic Domain to Orai1.” Cell 136.5 (2009): 876–890.

Penna, Aubin et al. “The CRAC Channel Consists of a Tetramer Formed by Stim-Induced Dimerization of Orai Dimers.” Nature 456.7218 (2008): 116–120.

Prakriya, Murali, and Richard S Lewis. “Store-Operated Calcium Channels.” Physiological reviews 95.4 (2015): 1383–436.

Ramsey, I Scott, Markus Delling, and David E Clapham. “An Introduction to TRP Channels.” Annual review of physiology 68 (2006): 619–647.

Schaballie, Heidi et al. “A Novel Hypomorphic Mutation in STIM1 Results in a Late-Onset Immunodeficiency.” The Journal of allergy and clinical immunology Sept. 2015: 816–819.e4.

Stanisz, Hedwig et al. “ORAI1 Ca2+ Channels Control Endothelin-1-Induced Mitogenesis and Melanogenesis in Primary Human Melanocytes.” The Journal of investigative dermatology 132.5 (2012): 1443–1451.

Stathopulos, Peter B et al. “STIM1/Orai1 Coiled-Coil Interplay in the Regulation of Store-Operated Calcium Entry.” Nature communications 4 (2013): 2963.

Stathopulos, Peter B et al. “Stored Ca2+ Depletion-Induced Oligomerization of Stromal Interaction Molecule 1 (STIM1) via the EF-SAM Region: An Initiation Mechanism for Capacitive Ca2+ Entry.” The Journal of biological chemistry 281.47 (2006): 35855–35862.

Stathopulos, Peter B. et al. “Structural and Mechanistic Insights into STIM1-Mediated Initiation of Store-Operated Calcium Entry.” Cell 135.1 (2008): 110–122.

Stiber, Jonathan et al. “STIM1 Signalling Controls Store-Operated Calcium Entry Required for Development and Contractile Function in Skeletal Muscle.” Nature cell biology 10.6 (2008): 688–697.

Stratton, Mr, Pj Campbell, and Pa Futreal. “The Cancer Genome.” Nature 458.7239 (2009): 719–724.

Vogelstein, Bert et al. “Cancer Genome Lanscapes.” Science 339.6127 (2013): 1546–1558.

Walker, D, and M De Waard. “Subunit Interaction Sites in Voltage-Dependent Ca2+ Channels: Role in Channel Function.” Trends in neurosciences 21.4 (1998): 148–154.

Wang, S et al. “STIM1 and SLC24A4 Are Critical for Enamel Maturation.” Journal of dental research 93.7 Suppl (2014): 94S–100S.

Yang, Shengyu, J. Jillian Zhang, and Xin Y. Huang. “Orai1 and STIM1 Are Critical for Breast Tumor Cell Migration and Metastasis.” Cancer Cell 15.2 (2009): 124–134.

Yang, Xue et al. “Structural and Mechanistic Insights into the Activation of Stromal Interaction Molecule 1 (STIM1).” Proceedings of the National Academy of Sciences of the United States of America 109.15 (2012): 5657–5662.

Yuan, Joseph P et al. “SOAR and the Polybasic STIM1 Domains Gate and Regulate Orai Channels.” Nature cell biology 11.3 (2009): 337–343.

Zhang, Shenyuan L et al. “Mutations in Orai1 Transmembrane Segment 1 Cause STIM1-Independent Activation of Orai1 Channels at Glycine 98 and Channel Closure at Arginine 91.” Proceedings of the National Academy of Sciences of the United States of America 108.43 (2011): 17838–17843.

Zhou, Yubin et al. “Pore Architecture of the ORAI1 Store-Operated Calcium Channel.” Proceedings of the National Academy of Sciences of the United States of America 107.11 (2010): 4896–4901.

Islam S., editor,. Transient receptor potential channels. Dordrecht: Springer, 2011.
ISBN 978-94-007-0264-6

Groschner, K., Graier W. F., Romanin C., Store-operated Ca2+ entry (SOCE) pathways: emerging signaling concepts in human (patho)physiology. New York: Springer, 2012.
ISBN 978-3-7091-0962-5